Structure:Function Relationships in Molecular Spin-Crossover Complexes

Malcolm A. Halcrow*

School of Chemistry, University of Leeds, Woodhouse Lane, Leeds, UK LS2 9JT.
E-mail: m.a.halcrow@leeds.ac.uk

Electronic Supplementary Information

Table S1. Structural data for salts of $[Fe(1\text{-bpp})_2]^{2+}$ and its derivatives. See below for schematics of the ligands in this Table, and the main text for the definitions of the four distortion parameters. Data are from ref. [1], unless otherwise stated.

	Spin-state behaviour	Spin-state of crystal structure	θ (º)	ϕ (º)	Σ (º)	Θ (º)
$[Fe(1\text{-bpp})_2][ClO_4]_2$	High-spin	High-spin	66.24(2)	155.7(1)	186.6(2)	547
$[Fe(1\text{-bpp})_2][PF_6]_2$	High-spin	High-spin	62.64(1)	154.18(7)	197.2(2)	559
$[Fe(1\text{-bpp})_2][SbF_6]_2$	High-spin	High-spin	61.94(2)	154.4(1)	199.0(3)	560
$[Fe(1\text{-bpp})_2][I_3]_2$	High-spin	High-spin	84.9(1)-88.7(1) [a]	156.4(4)- 171.1(5)[a]	155(1)- 172(1)[a]	479-514[a]
$[Fe(1\text{-bpp})_2]I_{0.5}[I_3]_{1.5}$	High-spin	High-spin	89.92(5)	156.0(2)	172.8(6)	522
$[Fe(1\text{-bpp})_2][Co(C_2B_9H_{11})_2]_2{\cdot}CH_3NO_2$, molecule A[b]	High-spin	High-spin	87.03(9)	159.6(3)	157(1)	482
$[Fe(\{3'\text{-Me}\}_2\text{-1-bpp})_2][SbF_6]_2$	High-spin	High-spin	87.66(4)	178.0(1)	148.8(4)	460
$[Fe(\{3'\text{-}i\text{Pr}\}_2\text{-1-bpp})_2][PF_6]_2{\cdot}CH_3CN{\cdot}0.5(C_2H_5)_2$	High-spin	High-spin	84.19(5)- 86.40(5)[c]	175.0(1)- 176.5(2)[c]	149.4(2)- 152.5(2)[c]	463-471[c]
$[Fe(\{3'\text{-}CO_2Et\}_2\text{-1-bpp})_2][BF_4]_2$	High-spin	High-spin	89.39(2)	174.62(7)	152.3(2)	479
$[Fe(4\text{-}\{CH{=}CH\text{ferrocenyl}\}\text{-1-bpp})_2][BF_4]_2{\cdot}2(C_2H_5)_2O$	High-spin	High-spin	88.3	175.4(2)	144.7(4)	453
α-$[Fe(\{3'\text{-Ph}\}_2\text{-1-bpp})_2][BF_4]_2$	High-spin	High-spin	61.15(4)	176.3(2)	177.0(7)	479
β-$[Fe(\{3'\text{-Ph}\}_2\text{-1-bpp})_2][BF_4]_2$	High-spin	High-spin	62.30(2)	180	176.8(2)	482
$[Fe(\{3'\text{-ferrocenyl}\}_2\text{-1-bpp})_2][BF_4]_2{\cdot}3CH_3CN$	High-spin	High-spin	66.3; 69.4[c]	180;180[c]	168; 169[c]	481; 479[c]
$[Fe(\{3'\text{-}CH_2OH\}_2\text{-1-bpp})_2][BF_4]_2$	High-spin	High-spin	72.08(3)	164.7(1)	166.3(3)	486
α-$[Fe(\{3'\text{-}CH_2OH\}_2\text{-1-bpp})_2][ClO_4]_2$	High-spin	High-spin	85.48(2)	164.86(8)	152.1(3)	474
β-$[Fe(\{3'\text{-}CH_2OH\}_2\text{-1-bpp})_2][ClO_4]_2$	High-spin	High-spin	71.56(2)	163.62(7)	172.3(2)	488
$[Fe(4\text{-}\{CH{=}CH\text{ferrocenyl}\}\text{-1-bpp})_2][I_3]_2$	High-spin	High-spin	85.7	163.4(3)	157(1)	491
$[Fe(4\text{-}\{CH{=}CH\text{ferrocenyl}\}\text{-1-bpp})_2][BPh_4]_2{\cdot}3CH_3NO_2{\cdot}(C_2H_5)_2O$	High-spin	High-spin	86.6	156.6(1)	167.7(5)	528
$[Fe(4\text{-}\{CH{=}CH\text{ferrocenyl}\}\text{-1-bpp})_2][Ni(mnt)_2]_2$	High-spin	High-spin	74.4	166.1(2)	169.7(7)	479
α-$[Fe(4\text{-}\{CH_2SCN\}\text{-1-bpp})_2][BF_4]_2$	High-spin	High-spin	78.8	158.10(7)	169.1(2)	486
$[Fe(bppyz)_2][SbF_6]_2$	High-spin	High-spin	59.84(3)	154.5(1)	201.8(4)	562
$[Fe(bppyz)_2][SbF_6]_2{\cdot}2CH_3NO_2$	High-spin	High-spin	84.66(4)	163.2(1)	161.0(5)	485
$[Fe(1\text{-bpp})_2][BF_4]_2$	Spin-crossover	High-spin	89.94(2)	172.98(7)	150.8(2)	467
		Low-spin	89.40(2)	178.15(8)	86.1(2)	282
$[Fe(1\text{-bpp})_2][BF_4]_2{\cdot}3CH_3NO_2$	Spin-crossover	Low-spin	86.34(4); 89.14(4)[d]	178.3(1); 177.5(1)[d]	89.1(4); 86.5(4)[d]	279; 283[d]
$[Fe(1\text{-bpp})_2][Ni(mnt)_2]_2{\cdot}CH_3NO_2$[2]	Spin-crossover	High-spin	76.7	178.4	157.9(5)	450
		Low-spin	81.3	177.9	94.1(5)	282
$[Fe(\{3'\text{-Me}\}_2\text{-1-bpp})_2][BF_4]_2$	Spin-crossover	High-spin	76.4	175.85(9)	153.1(3)	462
		Low-spin	81.9	179.2(2)	92.9(5)	285
$[Fe(\{3'\text{-Me}\}_2\text{-1-bpp})_2][BF_4]_2{\cdot}xH_2O$	Spin-crossover	High-spin	76.4	175.3(1)	154.8(4)	460
$[Fe(1\text{-bpp})_2][Co(C_2B_9H_{11})_2]_2{\cdot}CH_3NO_2$, molecule B[b]	Spin-crossover	Low-spin	87.4(1)	178.3(3)	87(1)	283
$[Fe(\{4'\text{-Me}\}_2\text{-1-bpp})_2][ClO_4]_2$	Spin-crossover	High-spin	90	180	158.8(4)	480
		Low-spin	89.9	175.8(4)	89(1)	288
$[Fe(1\text{-bip})_2][BF_4]_2{\cdot}1{+}x CH_3NO_2{\cdot}1{-}x(C_2H_5)_2O$	Spin-crossover	Low-spin	81.32(5)- 89.66(4)[e]	174.5(2)-178.7(2)[e]	80.1(7)-89.5(6)[e]	263-279[e]
α-$[Fe(\{4'\text{-Cl}\}_2\text{-1-bpp})_2][BF_4]_2$	Spin-crossover	High-spin	90	180	153.2(3)	470
		Low-spin	89.82(4)	176.9(3)	85.4(8)	280
$[Fe(\{4'\text{-Br}\}_2\text{-1-bpp})_2][BF_4]_2$	Spin-crossover	High-spin	90	180	150.9(2)	467

Table S1 continued

$[Fe(4\text{-}\{CH_2OH\}\text{-}1\text{-}bpp)_2][BF_4]_2$	Spin-crossover	High-spin	89.71(4)	178.4(1)	147.6(6)	454
		Low-spin	89.87(4)	177.3(2)	91.2(4)	297
$[Fe(4\text{-}\{CH_2OH\}\text{-}1\text{-}bpp)_2][ClO_4]_2$	Spin-crossover	High-spin	89.4	177.4(3)	147.7(9)	458
		Low-spin	90.0	177.7(4)	94(1)	306
β-$[Fe(4\text{-}\{CH_2SCN\}\text{-}1\text{-}bpp)_2][BF_4]_2$	Spin-crossover	High-spin	88.5	172.34(8)	147.3(3)	459
		Low-spin	88.7	178.22(6)	87.3(2)	286
$[Fe(4\text{-}NITR\text{-}1\text{-}bpp)_2][BF_4]_2\cdot(CH_3)_2CO$	Spin-crossover	Low-spin	89.8	178.2(3)	87(1)	284
$[Fe(4\text{-}I\text{-}1\text{-}bpp)_2][ClO_4]_2$	Spin-crossover	Low-spin	88.2	178.6(1)	86.1(4)	281
$[Fe(4\text{-}\{C{\equiv}CC_6H_4SC\{O\}Me\}\text{-}1\text{-}bpp)_2][ClO_4]_2$	Spin-crossover	Low-spin	88.0	177.7(2)	87.2(6)	285
$[Fe(4\text{-}\{C_6H_4OH\}\text{-}1\text{-}bpp)_2][ClO_4]_2$	Spin-crossover	Low-spin	87.7	178.3(1)	89.0(3)	291
catena-$[FeH(4\text{-}\{4\text{-pyridyl}\}\text{-}1\text{-}bpp)_2]_m[ClO_4]_{3m}\cdot m CH_3OH$	Spin-crossover	Low-spin	87.2	174.9(2)	88.0(7)	283
$[Fe(4\text{-}\{3\text{-pyridyl}\}\text{-}1\text{-}bpp)_2][BF_4]_2$ [3]	Spin-crossover	Low-spin	86.4	179.26(12)	87.1(4)	282
$[Fe(4\text{-}\{3\text{-pyridyl}\}\text{-}1\text{-}bpp)_2][ClO_4]_2$ [3]	Spin-crossover	Low-spin	84.7	179.0(2)	89.3(7)	284
$[FeH(4\text{-}\{3\text{-pyridyl}\}\text{-}1\text{-}bpp)_2]_m[BF_4]_{3m}\cdot m CH_3CN\cdot m H_2O$ [3]	Spin-crossover	Low-spin	88.2	173.92(13)	86.6(5)	285
$[Fe(bppyz)_2][BF_4]_2\cdot 3CH_3NO_2$	Spin-crossover	High-spin	86.42(4)	173.2(1)	153.6(4)	476
		Low-spin	86.24(3)	177.4(1)	91.5(4)	296
$[Fe(\{3'\text{-}Me\}_2\text{-}bppyz)_2][BF_4]_2$	Spin-crossover	High-spin	90	180	150.3(2)	460
		Low-spin	90	180	94.0(2)	309
$[Fe(\{3'\text{-}Me\}_2\text{-}bppyz)_2][ClO_4]_2$	Spin-crossover	High-spin	90	180	156.1(2)	480
		Low-spin	90	180	96.1(2)	316
$[Fe(\{3',5'\text{-}Me_2\}\text{-}1\text{-}bpp)_2][BF_4]_2$	Low-spin	Low-spin	84.18(2)	176.96(7)	85.2(2)	272
$[Fe(\{4'\text{-}Me\}_2\text{-}1\text{-}bpp)_2][BF_4]_2$	Low-spin	Low-spin	89.90(3)	178.0(1)	84.3(4)	276
$[Fe(\{3'\text{-}Mes\}_2\text{-}1\text{-}bpp)_2][PF_6]_2\cdot 2CH_3NO_2$	Low-spin	Low-spin	89.50(2)	178.98(8)	84.0(3)	277
$[Fe(\{3'\text{-}Mes\}_2\text{-}1\text{-}bpp)_2][FeCl_4]_2$	Low-spin	Low-spin	89.9	178.7(3)	81(1)	269
$[Fe(\{4'\text{-}CO_2Et\}_2\text{-}1\text{-}bpp)_2][BF_4]_2\cdot 2CF_3C_2OH$	Low-spin	Low-spin	85.52(3)	176.4(1)	83.3(3)	272
$[Fe(\{4'\text{-}I\}_2\text{-}1\text{-}bpp)_2][BF_4]_2\cdot 2(CH_3)_2CO$	Low-spin	Low-spin	89.02(4)	175.5(2)	86.8(5)	284
$[Fe(4\text{-}\{CH_2N[CH_2\text{-}2\text{-pyridyl}]_2PdCl\}\text{-}1\text{-}bpp)_2][BF_4]_4$ $\cdot 6.8CH_3NO_2\cdot 0.3(C_2H_5)_2O$ [4]	n/a	Low-spin	86.69(4)	177.69(13)	86.7(4)	284
$[Fe(bppyz)_2][SbF_6]_2\cdot 3CH_3NO_2$	n/a	Low-spin	88.59(4)	178.6(2)	85.5(5)	281
$[Fe(\{3',5'\text{-}Me_2\}_2\text{-}bppyz)_2][BF_4]_2$	Low-spin	Low-spin	88.09(3); 89.87(3)[d]	176.1(1); 179.5(1)[d]	84.5(4); 86.8(4)[d]	279; 285[d]
$[Fe(\{3'\text{-}Mes\}_2\text{-}bppyz)_2][BF_4]_2\cdot 5CH_3NO_2$	Low-spin	Low-spin	82.09(4)	179.8(2)	95.9(3)	288

[a]There are six unique molecules in the asymmetric unit of this compound, all in the same spin state. [b]There are two unique molecules in the asymmetric unit of this material, which have different spin-state behaviour. [c]There are four unique molecules in the asymmetric unit of this compound, all in the same spin state. [d]There are two unique molecules in the asymmetric unit of this compound, both in the same spin state. [e]There are three unique molecules in the asymmetric unit of this compound, all in the same spin state.

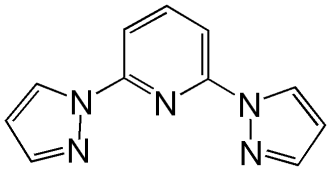

1-bpp

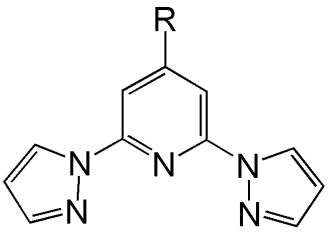

4-R-1-bpp

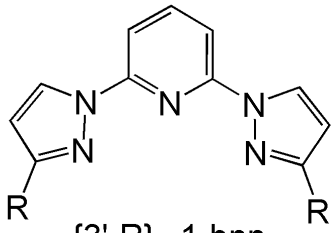

{3'-R}$_2$-1-bpp

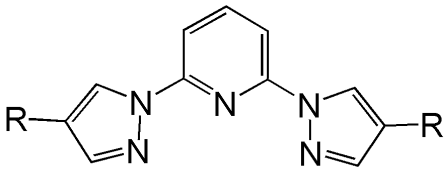

{4'-R}$_2$-1-bpp

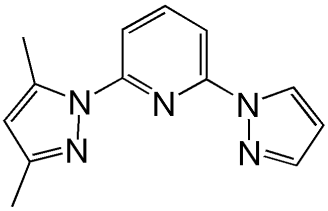

{3',5'-Me$_2$}-1-bpp

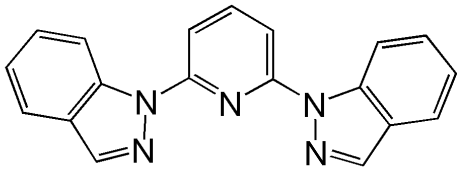

1-bip

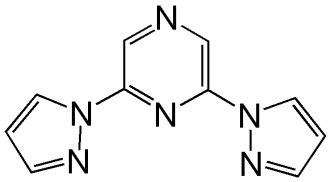

bppyz

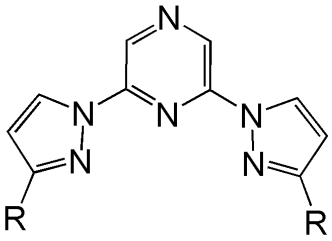

{3'-R}$_2$-bppyz

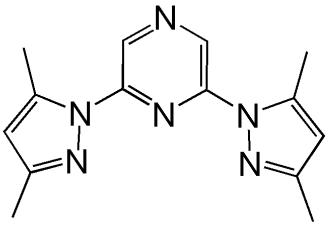

{3',5'-Me$_2$}$_2$-bppyz

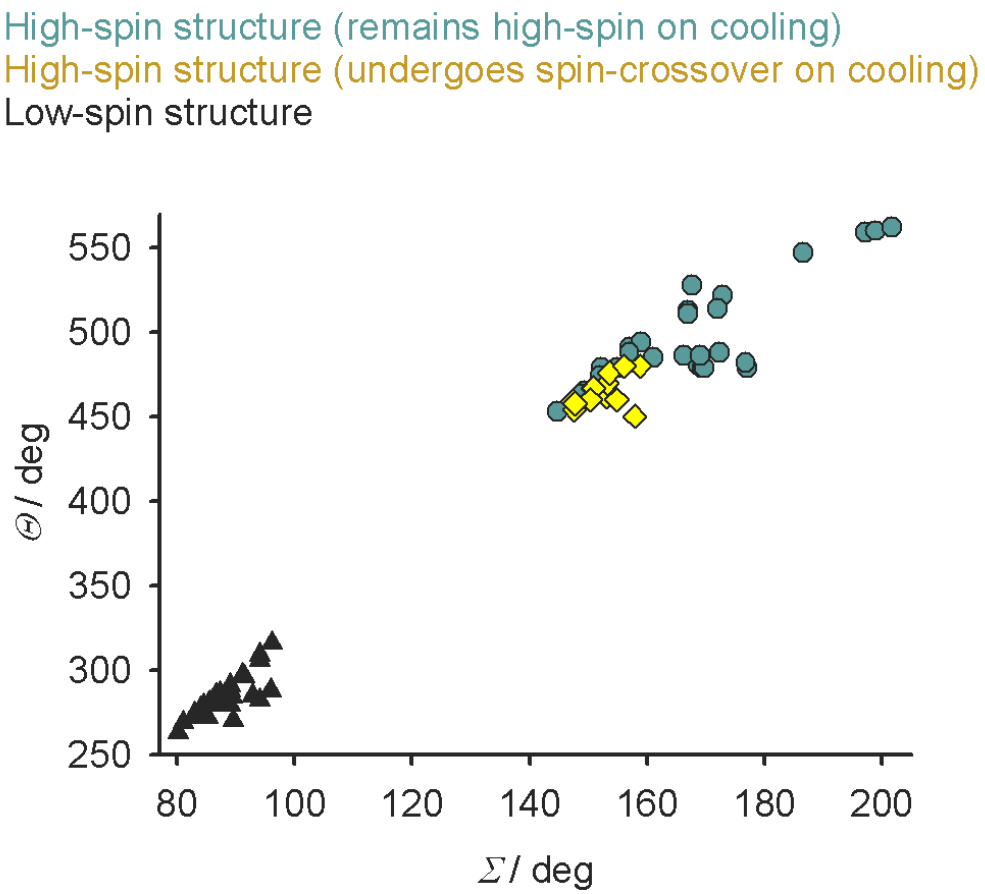

Figure S1. Plot of Σ *vs.* Θ for crystallographically characterised complexes from the $[Fe(1\text{-bpp})_2]^{2+}$ series (Table S1).

Complexes that are spin-crossover active clearly exhibit Σ and Θ values towards the low end of the range observed for the high-spin state of $[Fe(1\text{-bpp})_2]^{2+}$ compounds. This correlates with the angular Jahn-Teller distortion exhibited by this series of high-spin complex. See the main text for more details.

Table S2. Structural changes taking place during spin-crossover for $[Fe(1\text{-bpp})_2]^{2+}$ and its derivatives, whose high-spin and low-spin crystal structures are available (Table S1, Fig. S1). Data are taken from ref. [1] unless otherwise stated.

	$T_{½}$ (K)	ΔT (K)	$\lvert\Delta\theta\rvert$ (º)	$\lvert\Delta\phi\rvert$ (º)	$\Delta\Sigma$ (º)	$\Delta\Theta$ (º)
$[Fe(1\text{-bpp})_2][BF_4]_2$	260	3	0.5	5.2	64.7	185
$[Fe(1\text{-bpp})_2][Ni(mnt)_2]_2{\cdot}CH_3NO_2$[2]	170	0-70	4.5	0.5	63.8	168
$[Fe(\{3'\text{-}Me_2\}\text{-}1\text{-bpp})_2][BF_4]_2$	147	6	5.5	3.4	60.2	177
$[Fe(\{4'\text{-}Me_2\}\text{-}1\text{-bpp})_2]\ [ClO_4]_2$	233	3	0.14	4.2	69.8	192
α-$[Fe(\{4'\text{-}Cl_2\}\text{-}1\text{-bpp})_2][BF_4]_2$	202	3	0.18	3.1	67.8	190
$[Fe(4\text{-}\{CH_2OH\}\text{-}1\text{-bpp})_2][BF_4]_2$	271	0	0.16	1.13	56.4	157
$[Fe(4\text{-}\{CH_2OH\}\text{-}1\text{-bpp})_2][ClO_4]_2$	284	0	0.62	0.3	53.7	152
β-$[Fe(4\text{-}\{CH_2SCN\}\text{-}1\text{-bpp})_2][BF_4]_2$	272	0	0.2	5.9	60.0	173
$[Fe(bppyz)_2][BF_4]_2{\cdot}3CH_3NO_2$	198	n/a	0.18	4.2	62.1	180
$[Fe(\{3'\text{-}Me_2\}\text{-}1\text{-bppyz})_2][BF_4]_2$	240	0	0	0	56.3	151
$[Fe(\{3'\text{-}Me_2\}\text{-}1\text{-bppyz})_2][ClO_4]_2$	190	0	0	0	60.0	164

Table S3 Structural data for iron(II) complexes of *tris*-pyrazolylborates and related ligands. See below for schematics of the ligands in this Table, and the main text for the definitions of Σ and Θ. Data are from ref. [5], unless otherwise stated.

	Spin-state behaviour	Spin-state of crystal structure	Fe–*N2–N1–C5* (average, °)	Fe–*N2–N1*–B (average, °)	Σ (°)	Θ (°)
$[Fe(pz^{Me3}{}_3BH)_2]$	High-spin	High-spin	162.4	20.2	43.3(2)	57
$[Fe(pz^{CF3}{}_3BH)_2]$	High-spin	High-spin	178.3	1.0	22.7(3)	29
$[Fe(pz^{cPr}{}_4B)_2]\cdot CH_3OH$, molecule 1[a]	High-spin	High-spin	166.3	9.3	45.60(14)	62
$[Fe(PhBpz^{Me}{}_3)_2]$	High-spin	High-spin	162.1	12.9	46.96(14)	66
$[Fe(pz^{Me}{}_3BC_6H_4I)_2]$, nSCO polymorph	High-spin	High-spin	164.9	9.3	48.5(2)	66
$[Fe(pz^{Ph}{}_3BH)_2]$	n/a	High-spin	174.2	7.3	48.3(3)	158
$[Fe(pz^{Me}{}_4B)_2]$[6]	n/a	High-spin	169.3	7.3	47.6(3)	58
$[Fe(pz^{cPr}{}_4B)_2]\cdot ½C_7H_8$	n/a	High-spin	168.7; 168.9[b]	9.0; 11.7[b]	47.2(3); 48.4(3)[b]	59; 59[b]
$[Fe(pz^{Ph,4\text{-}CN}{}_2pz^{5\text{-}Ph,4\text{-}CN}BH)_2]$[7]	n/a	High-spin	175.6	10.8	49(1)	91
$[Fe(pz^{Me}{}_3BH)_2]$	Spin-crossover	High-spin	176.7; 178.3[b]	3.5; 0.5[b]	43.6(8); 42.0(7)[b]	50; 49
$[Fe(pz^{*}{}_3BH)_2]$	Spin-crossover	High-spin	174.2	6.8	41.2(3)	51
$[Fe(pz^{cyPr}{}_3BH)_2]$	Spin-crossover	High-spin	179.1	0.3	46.8(5)	54
$[Fe(pz^{Me}{}_3BC_6H_4CCSiMe_3)_2]$	Spin-crossover	High-spin	165.4	7.9	38.2(4)	56
$[Fe(pz^{Me}{}_3BC_6H_4CCPh)_2]$	Spin-crossover	High-spin	164.7	10.5	47.5(2)	64
$[Fe(pz^{cPr}{}_4B)_2]\cdot CH_3OH$, molecule 2[a]	Spin-crossover	High-spin	171.0	5.5	48.0(2)	61
		Low-spin	174.8	5.7	5.60(14)	9
$[Fe(pz^{Me}{}_3BC_6H_4I)_2]$, SCO polymorph	Spin-crossover	High-spin	166.1	8.6	44.5(2)	64
		Low-spin	171.8	4.8	4.2(3)	11
$[Fe(pz^{Me}{}_3BC_6H_4I)_2]\cdot 2CH_2Cl_2$	Spin-crossover	High-spin	164.4	9.8	48.0(3)	60
		Low-spin	171.2	5.3	6.2(2)	10
$[Fe(pz^{Me}{}_3BC_6H_4CCH)_2]$	Spin-crossover	~80% High-spin	163.5; 170.2[c]	9.3; 6.0[c]	37.5(2); 28.5(2)[b]	52;38[b]
		Low-spin	169.8; 172.1[b]	4.8; 5.2[b]	3.0(2); 3.3(2)[b]	8, 9[b]
$[Fe(pz_3BH)_2]$, low temperature phase	Spin-crossover	Low-spin	177.5; 179.1[b]	2.9; 0.8[b]	26.4(7); 21.2(6)[b]	25;25[b]
$[Fe(pz_3BH)_2]$, annealed phase[8]	Spin-crossover	*ca.* 80% High-spin	176.0	1.3	44.5(5)	68
		Low-spin	175.9	1.3	19.2(2)	30
$[Fe(pz^{Me}{}_3B\textit{t}Bu)_2]$[9]	Spin-crossover	Low-spin	178.1(2)	2.0(3)	6.1(2)	7
$[Fe(pz_4B)_2]$	Low-spin	Low-spin	172.5; 175.1[b]	1.7; 3.0[b]	16.8(7); 20.4(7)[b]	21; 25[b]
$[Fe(pz_3BPh)_2]$	Low-spin	Low-spin	171.3	5.3	42(1)	30
$[Fe(pz_3BC_6H_4I)_2]$	Low-spin	Low-spin	172.6	5.0	20.2(3)	25
$[Fe(in_3BH)_2]\cdot 3.5CHCl_3$[10]	Low-spin	Low-spin	174.9; 175.8[b]	6.9; 5.3[b]	20(1); 14(1)[b]	26;18[b]
$[Fe(pz_3B\textit{t}Bu)_2]$[9]	Low-spin	Low-spin	177.02(12)	4.38(18)	28.92(16)	33

[a] There are two unique molecules in the asymmetric unit of this material, which have different spin-state behaviour. [b]There are two unique molecules in the asymmetric unit of this compound, both in the same spin state. [c]There are two unique molecules in the asymmetric unit of this crystal phase, one of which is high-spin while the other is *ca.* 60% high-spin at this temperature.

Table S4 Structural data for iron(II) complexes of *tris*-pyrazolylmethane and *tris*-pyrazolylmethanide ligands. See below for schematics of the ligands in this Table, and the main text for the definitions of Σ and Θ.

	Spin-state behaviour	Spin-state of crystal structure	Fe–*N2*–*N1*–*C5* (average, °)	Fe–*N2*–*N1*–X (average, °)	Σ (°)	Θ (°)
$[Fe(pz^*_3CH)_2]I_2{\cdot}4CH_2Cl_2$[11]	High-spin	High-spin	162.1(3)	17.7(3)	65.5(3)	76
$[Fe(pz^{Me3}_3CH)_2]I_2{\cdot}4CH_2Cl_2$[12]	n/a	High-spin	171.8	5.8	67.6	82
$[Fe(pz^*_3CH)_2][Fe_2OCl_6]$[13]	n/a	High-spin	178.9	3.1(9)	65.8(6)	75
$[Fe(pz^*_3CH)_2][BF_4]_2$, high-T phase[14]	Spin-crossover	High-spin	168.0(3)	12.5(3)	67.2(3)	81
$[Fe(pz^*_3CH)_2][BF_4]_2$, low-T phase, molecule 1[a] [14]	High-spin	High-spin	161.7(3)	20.2(3)	64.0(3)	78
$[Fe(pz^*_3CH)_2][BF_4]_2$, low-T phase, molecule 2[a] [14]	Low-spin	Low-spin	179.0(3)	1.3(3)	19.2(3)	23
$[Fe(pz^*_3CH)_2]I_2$[11]	Spin-crossover	High-spin	171.2(5)	8.7(5)	65.4(5)	79
$[Fe(pz^*_3C)_2]{\cdot}2thf$ [15]	Spin-crossover	High-spin	n/a[b]	n/a[b]	64.8(3)	n/a[b]
		Low-spin	177.4	2.9	22.9(3)	29
$[Fe(pz^{Me}_2pz^{5\text{-}Me}CH)_2][BF_4]_2$[16]	Spin-crossover	*ca.* 70% High-spin	177.0(9)	2.2(9)	63.4(6)	71
		Low-spin	177.8(6)	1.6(6)	26.0(3)	31
$[Fe(pz^{Me3}_3CH)_2][BF_4]_2$[17]	Spin-crossover	High-spin	174.4(3)	n/a[b]	70.3(3)	n/a[b]
$[Fe(pz^*_3CH)(pz_3CH)][BF_4]_2$, polymorph A[18]	Spin-crossover	Low-spin	178.5(7)	1.4(7)	23.3(5)	30
$[Fe(pz^*_3CH)(pz_3CH)][BF_4]_2$, polymorph B[18]	Spin-crossover	High-spin	172.1(5)	6.0(5)	66.3(3)	77
		Low-spin	176.4(4)	1.7(4)	24.8(3)	30
$[Fe(pz^*_3CH)(pz^{4\text{-}Me}_3CH)][BF_4]_2{\cdot}2CH_3CN$[18]	Spin-crossover	High-spin	172.3	7.3	70.7(3)	81
		Low-spin	174.6	5.8	34.4(3)	44
$[Fe(pz^*_3CH)(pz_3CCH_2OH)][BF_4]_2$[18]	Spin-crossover	Low-spin	176.5(4)	1.1(4)	24.3(3)	33
$[Fe(pz_3CH)_2][NO_3]_2$, α-polymorph[19]	Spin-crossover	Low-spin	177.8	2.1	28.8(3)	34
$[Fe(pz_3CH)_2][NO_3]_2$, β-polymorph[19]	Spin-crossover	Low-spin	177.9	1.9	29.0(3)	35
$[Fe(pz_3CH)_2][BF_4]_2$[20]	Low-spin	Low-spin	178.4	0.5	30.6(4)	38
$[Fe(pz_3CH)_2][Fe(NCS)_5(py)]{\cdot}2CH_3CN$[21]	n/a	Low-spin	177.5(3); 178.3(3)[b]	0.3(3); 2.3(3)[b]	29.9(2); 31.2(2)[b]	35; 37[b]
$[Fe(pz_3CCH_2OP\{O\}Ph_2)_2][BF_4]_2$[22]	n/a	Low-spin	176.0	2.9	30.4(2)	37
$[\{Fe(pz^*_3CH)\}_2(\mu\text{-}\{pz_3CCH_2OCH_2\}_2C_6H_4)][BF_4]_4$[23]	n/a	Low-spin	177.6	1.8	24.3(4)	32

[a]There are two unique molecules in the asymmetric unit of this phase, which have different spin-state behaviour. [b]The published high-spin structure of this compound is not available on the Cambridge Crystallographic Database. Therefore, these data could not be calculated. [c]There are two unique molecules in the asymmetric unit of this compound, both in the same spin state.

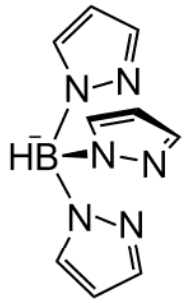

pz_3BH^-

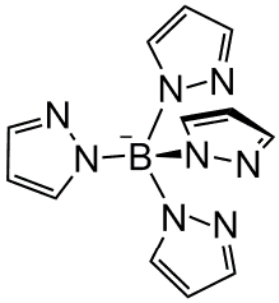

pz_4B^-

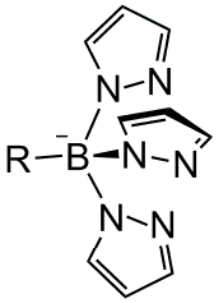

pz_3BR^-

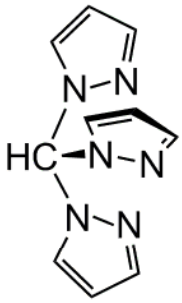

pz_3CH

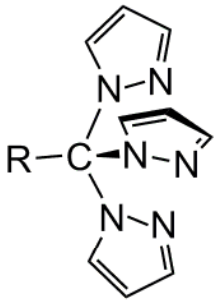

pz_3CR

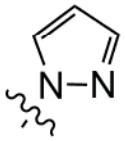

pz

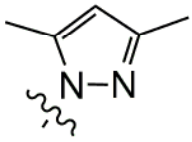

pz*

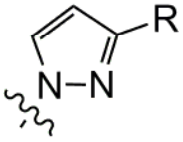

pz^R

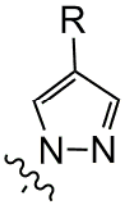

$pz^{4\text{-}R}$

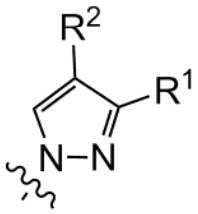

$pz^{R_1,4\text{-}R_2}$

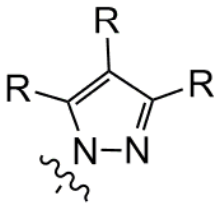

pz^{R3}

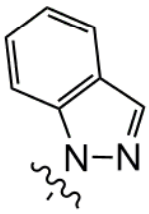

in

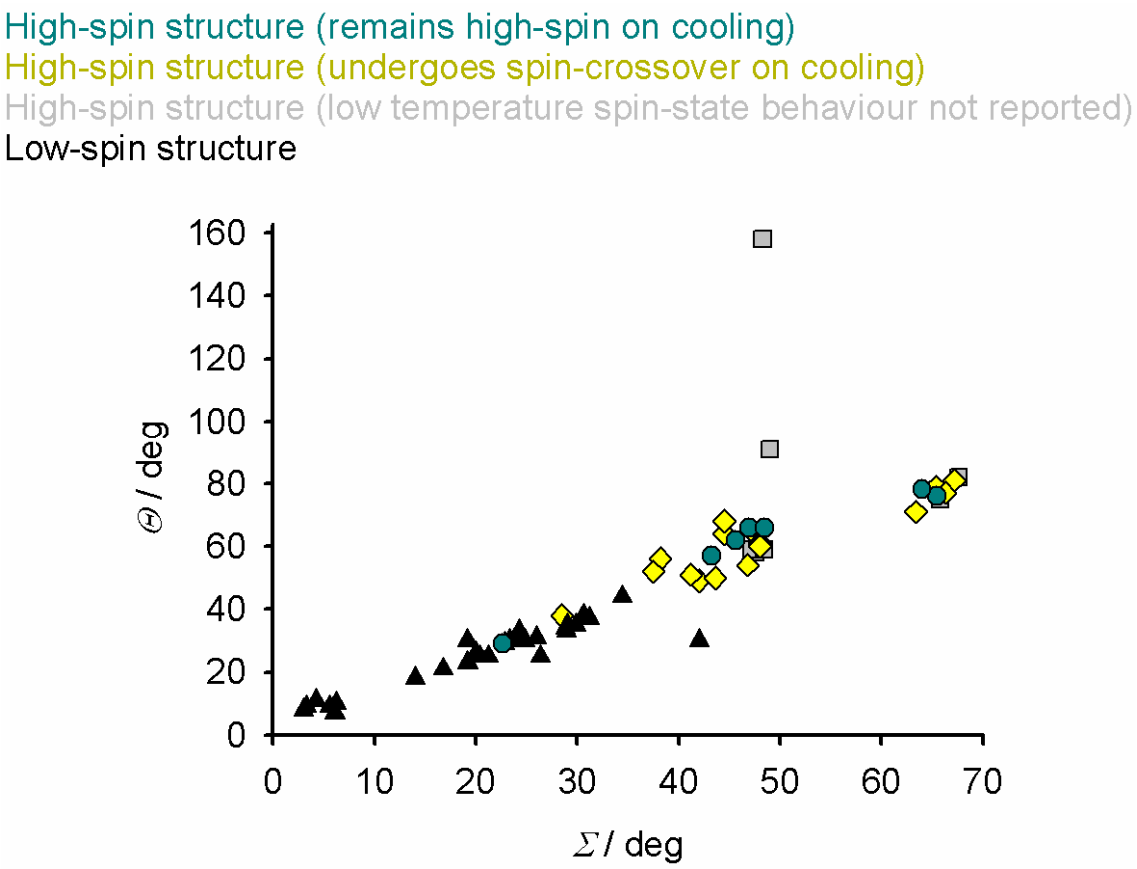

Figure S2. Plot of Σ *vs.* Θ for crystallographically characterised iron(II) scorpionate complexes (Tables S3 and S4).

The range of Σ and Θ values shown by these compounds is much narrower than for the other compounds examined in this work. That reflects the six-membered chelate rings formed by the tripodal scorpionate ligands, which favour *cis*-N–Fe–N bond angles close to 90°.

There is no apparent correlation between Σ and Θ and the occurence of spin-crossover in these compounds. See the main text for a discussion of the dependence of spin-crossover on the scorpionate ligand conformation.

The two outlying datapoints with abnormally high values of Θ are both pyrazolylborate complexes with 3-phenyl substituents at their pyrazole rings, which exert a strong steric influence on the metal coordination sphere. These are both probably high-spin compounds, although their spin-states at low temperature were not recorded.

Table S5 Structural changes taking place during spin-crossover for iron(II) complexes of scorpionate ligands, whose high-spin and low-spin crystal structures are available.

	$T_{½}$ (K)	ΔT (K)	|Δ Fe–*N2–N1–C5* | (º)	|Δ Fe–*N2–N1*–X | (º)	$\Delta\Theta$ (º)
$[Fe(Bpz^{cPr}{}_4)_2]\cdot CH_3OH$, molecule 2[5]	175	n/a	3.8	0.2	52
$[Fe(IC_6H_4Bpz^{Me}{}_3)_2]$, SCO polymorph[5]	130	n/a	5.7	3.8	53
$[Fe(IC_6H_4Bpz^{Me}{}_3)_2]\cdot 2CH_2Cl_2$[5]	175	n/a	6.8	4.5	50
$[Fe(HCpz^*{}_3)(HCpz_3)][BF_4]_2$, polymorph B[18]	228	0	4.3	4.3	47
$[Fe(HCpz^*{}_3)(HCpz^{4\text{-}Me}{}_3)][BF_4]_2\cdot 2CH_3CN$[18]	100[a]	0	2.3	1.5	37

[a]Transition proceeds in two closely-spaced steps, in a material with just one unique iron site. The $T_{½}$ value is the temperature where the transition has proceed to 50% completion in the material as a whole.

Table S6 Structural data for iron(III) $[Fe(saltrien)]^+$ derivatives. See below for schematics of the ligands in this Table, and the main text for the definitions of α, Σ and Θ. Data are taken from ref. [24], unless otherwise stated.

	Spin-state behaviour	Spin-state of crystal structure	α (°)	Σ (°)	Θ (°)
[Fe(saltrien)]BF_4 [25]	High-spin	High-spin	104.0(1)	95.7(3)	249
[Fe(saltrien)]PF_6	High-spin	High-spin	114.55(12); 121.08(13)[a]	95.0(5); 105.0(5) [a]	236; 323[a]
[Fe(saltrien)]BPh_4·½$(CH_3)_2CO$	High-spin	High-spin	124.98(6)	94.1(2)	239
[Fe(saltrien)]BPh_4·½$C_2H_4Cl_2$	High-spin	High-spin	121.80(9)	95.5(3)	240
[Fe(saltrien)]ClO_4, molecule A[b]	High-spin	High-spin	76.6(3)	96.0(6)	254
[Fe(saltrien)][$MnCr(C_2O_4)_3$]·CH_3OH [26]	High-spin	High-spin[b]	103.0(8); 120.1(7)[a]	71(2); 89(2)[a]	198; 230[a]
[Fe(5-OMe-saltrien)]PF_6·½H_2O	High-spin	High-spin	124.0	85.5(14)	204
[Fe(5-Me-saltrien)]PF_6,	High-spin	High-spin	98.69(4); 100.94(5)[a]	93.9(2); 118.8(2)[a]	244; 358[a]
[Fe(5-*t*Bu-saltrien)]NO_3·$C_2H_4Cl_2$	High-spin above 100 K	High-spin	108.80(6)	109.4(2)	284
[Fe(saltrien)][Ni$(dmit)_2$], monoclinic polymorph[c] [27]	High-spin	High-spin	118.0	91.4(4)	225
[Fe(saltrien)][Ni$(dcbdt)_2$]	*ca.* 85% High-spin	*ca.* 85% High-spin	79.9	56.9(4)	187
[Fe(saltrien)][Ni$(dmit)_2$], triclinic polymorph	Spin-crossover	High-spin	106.9	96.9(4)	250
		Low-spin	72.9	40.3(5)	56
[Fe(*N*{hexyl}saltrien)]BF_4, molecule 1[d] [25]	High-spin	High-spin	85.1(2)	81.8(5)	208
[Fe(*N*{hexyl}saltrien)]BF_4, molecule 2[d] [25]	Spin-crossover	*ca.* 50% High-spin	86.3(2)	67.2(5)	186
		Low-spin	86.3(1)	65.0(3)	140
[Fe(3,5-Cl_2-saltrien)]PF_6	Spin-crossover	High-spin	89.2	89(2)	263
[Fe(3,5-Cl_2-saltrien)]ClO_4	Spin-crossover	*ca.* 60% High-spin	88.1	68.7(6)	199
[Fe(saltrien)]BPh_4·$(CH_3)_2CO$	Spin-crossover	*ca.* 40% High-spin	85.8	50.1(7)	117
[Fe(5-OMe-saltrien)]ClO_4	n/a	*ca.* 10% High-spin	73.2	49.0(11)	94
[Fe(saltrien)][$MnCr(C_2O_4)_3$]·CH_2Cl_2 [26]	Spin-crossover	Low-spin	71.65(13)	51.6(6)	102
[Fe(saltrien)]ClO_4, molecule B[b]	Low-spin	Low-spin	73.6(2)	46.3(7)	83
[Fe(saltrien)]Cl·$2H_2O$	Low-spin	Low-spin	64.8	43.4(2)	69
[Fe(saltrien)]Br·H_2O	Low-spin	Low-spin	65.6	45.1(7)	71
[Fe(saltrien)]NO_3·H_2O	Low-spin	Low-spin	64.2	46.9(3)	74
[Fe(saltrien)][Ni$(dmit)_2$]·$(CH_3)_2CO$[c] [27]	Low-spin	Low-spin	72.5	50.2	86
[Fe(5-Cl-saltrien)]ClO_4	Low-spin ?	Low-spin	69.2	45.6(7)	79
[Fe(naphthtrien)]PF_6·$(C_2H_5)_2O$	Low-spin	Low-spin	61.83(6)	43.5(4)	98

[a]There are two unique molecules in the asymmetric unit of this compound, that are both in the same spin state. [b]There are three unique molecules in the asymmetric unit of this material, which have different spin-state behaviour. [c]Two other crystal forms of [Fe(saltrien)][Ni$(dmit)_2$] are also presented in ref. [27], but these were not spectroscopically or magnetochemically characterised. [d]There are two unique molecules in the asymmetric unit of this material, which have different spin-state behaviour.

Table S7 Structural data for iron(II) [Fe(5-NO_2-saltrien)] derivatives. See the main text for the definitions of α, Σ and Θ.

	Spin-state behaviour	Spin-state of crystal structure	α (°)	Σ (°)	Θ (°)
[Fe(5-NO_2-saltrien)][28]	Spin-crossover	High-spin	94.5	98.8(7)	247
		Low-spin ?[a]	92.4; 94.3[a]	97(3); 67(3)[a]	237; 100[a]
[Fe(3-OMe-5-NO_2-saltrien)][29]	Spin-crossover	High-spin	109.5	103.3(3)	290
		Low-spin	111.0	69.2(5)	198
[Fe(3-OEt-5-NO_2-saltrien)]·thf[29]	Partial spin-crossover[b]	High-spin	84.9	110.1(7)	315
[Fe(3-OMe-5-NO_2-*N*Me-saltrien)][30]	Partial spin-crossover[b]	High-spin	115.1	90.5(5)	231

[a]There are two unique molecules in the asymmetric unit of this compound, that should both be in a low-spin state according to magnetic susceptibility data. However, the Σ and Θ values imply that one molecule may be low-spin, and the other high-spin, in the single crystal at the temperature of measurement (103 K). [b]These compounds remain predominantly high-spin on cooling but show evidence of spin-crossover involving a fraction of the sample

Table S8 Structural data for iron(III) $[Fe(saltrien)]^+$ derivatives bearing an expanded chelate ring between the ligand amino donors. See below for schematics of the ligands in this Table, and the main text for the definitions of α, Σ and Θ.

	Spin-state behaviour	Spin-state of crystal structure	α (°)	Σ (°)	Θ (°)
[Fe(232-tet)]ClO_4[31]	High-spin above 78 K	High-spin	108.4	116.5(4)	344
[Fe(3-OMe-232-tet)]ClO_4[31]	High-spin above 78 K	High-spin	97.3	84(1)	238
[Fe(3,5-{OMe}$_2$-232-tet)]ClO_4 high-T phase[a] [32]	Spin-crossover	High-spin	111.9	74.7(4)	216
[Fe(3,5-{OMe}$_2$-232-tet)]ClO_4 mixed-spin phase, molecule 1[a] [32]	Spin-crossover	High-spin	107.6	87.5(5)	250
[Fe(3,5-{OMe}$_2$-232-tet)]ClO_4 mixed-spin phase, molecule 1[a] [32]	Low-spin	Low-spin	115.7	54.1(5)	90

[a]There are two unique molecules in the asymmetric unit of this phase, which have different spin-state behaviour.

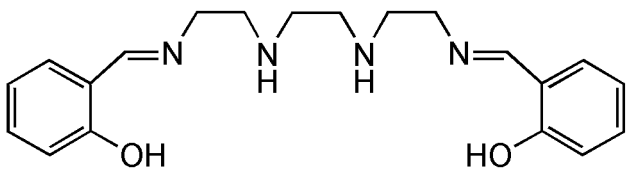

H_2saltrien

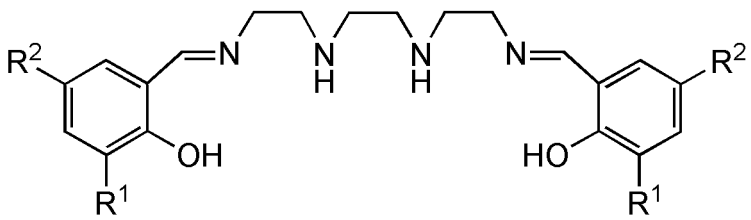

H_2(3-R^1-5-R^2-saltrien)

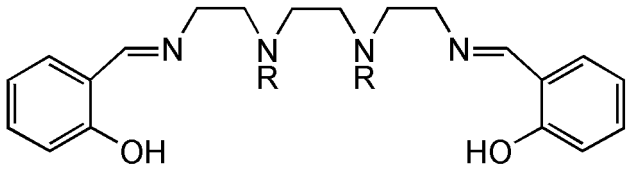

H_2(*N*R-saltrien)

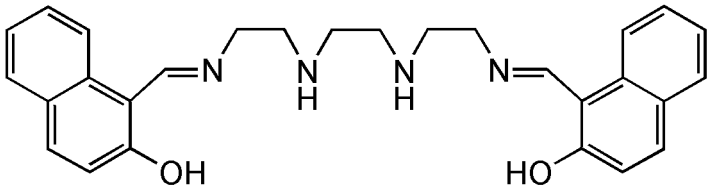

H_2naphthtrien

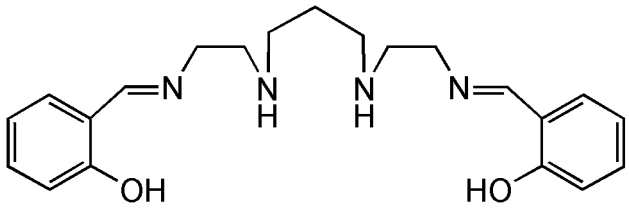

H_2(2,3,2-tet)

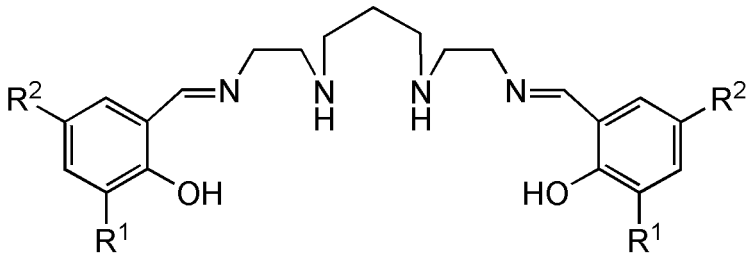

H_2(3-R^1-5-R^2-2,3,2-tet)

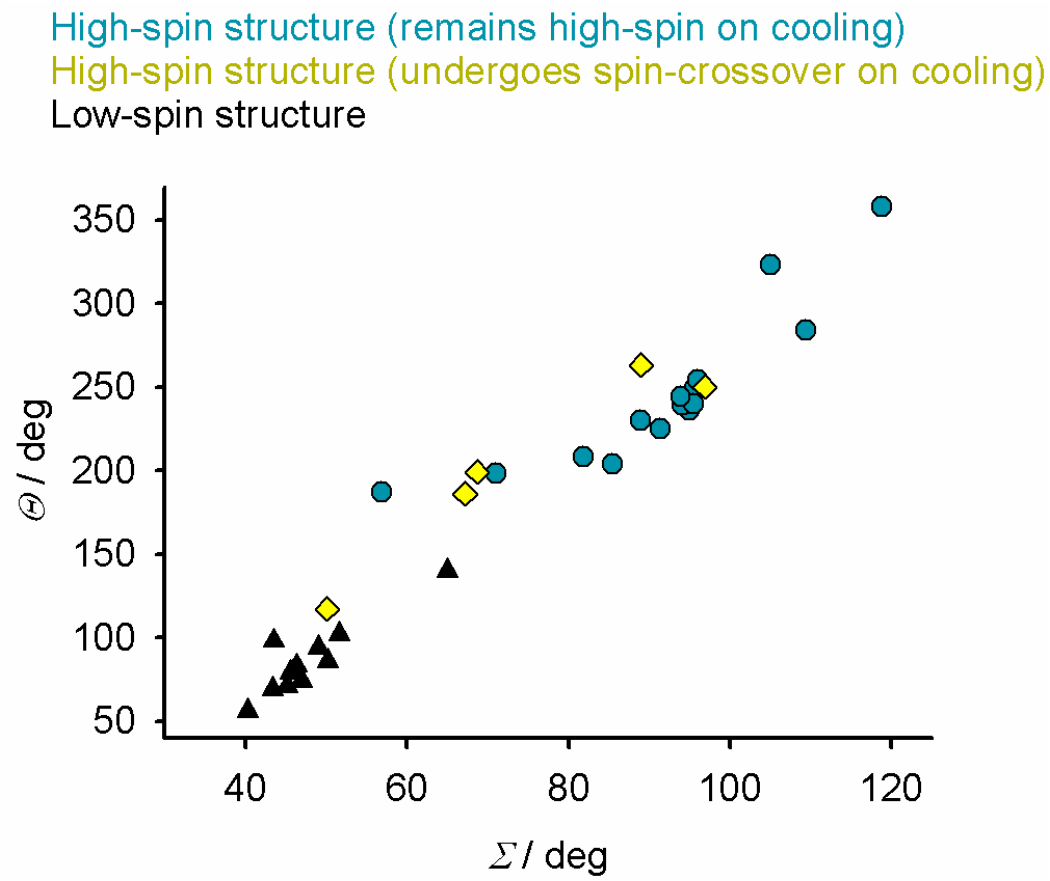

Figure S3. Plot of Σ *vs.* Θ for crystallographically characterised complexes from the $[Fe(saltrien)]^+$ series (Table S6).

There is no apparent correlation between Σ and Θ and the occurence of spin-crossover in these compounds. See the main text for a discussion of the dependence of spin-crossover on the saltrien ligand conformation.

Table S9 Structural data for iron(III) complexes of pap$^-$, qsal$^-$ and related tridentate Schiff base derivatives. See the next page for schematics of the ligands in this Table, and the main text for the definitions of θ, ϕ, Σ and Θ.

	Spin-state behaviour	Spin-state of crystal structure	θ (°)	ϕ (°)	Σ (°)	Θ (°)
$[Fe(qsal)_2][Ni(pddt)_2]$[33]	High-spin	High-spin	66.8	168.69(9)	75.3(3)	210
$[Fe(qsal)_2][Cu(pds)_2]$[34]	High-spin	High-spin	70.5	162.64(12)	81.2(4)	234
$[Fe(qsal)_2][Au(pds)_2]$[34]	High-spin	High-spin	70.7	162.3(2)	84.6(7)	231
$[Fe(pap)_2]BF_4 \cdot H_2O$[a] [35]	High-spin	High-spin	87.2	162.4	120.6	369
$[Fe(pap)_2]ClO_4 \cdot H_2O$[a] [36]	High-spin	High-spin	85.9	164.0(3)	117(1)	357
$[Fe(pap)_2]PF_6 \cdot CH_3OH$[37]	Spin-crossover	Low-spin	n/a[b]	176.4(2)	58.2(7)	n/a[b]
$[Fe(qsal)_2]NCS$[35]	Spin-crossover	High-spin	83.1	170.5	65.3	180
$[Fe(qsal)_2]NCS \cdot CH_2Cl_2$[35]	n/a	Low-spin	85.5	178.0	49.8	76
$[Fe(qsal)_2]NCSe$[35]	Spin-crossover	High-spin	79.5; 82.6[c]	169.2; 169.9[c]	69.9; 74.4[c]	204; 202[c]
$[Fe(qsal)_2]NCSe \cdot MeOH$[38]	Spin-crossover	Low-spin	n/a	179.0(3)	51(1)	n/a
$[Fe(qsal)_2]NCSe \cdot CH_2Cl_2$[38]	Spin-crossover	Low-spin	80.6	178.3(1)	49.9(3)	81
$[Fe(qsal)_2][Ni(dmit)_2]$[39]	Partial spin-crossover	High-spin	77.7	168.4	69.7	200
		ca. 55% High-spin	76.9	170.5	54.7	152
$[Fe(qsal)_2][Ni(dmit)_2] \cdot x CH_3CN$[40]	Spin-crossover	High-spin	89.8	166.21(9)	72.7(3)	203
		Low-spin	87.9	176.5	44.8	66
$[Fe(qsal)_2][Ni(dmit)_2]_3 \cdot CH_3CN \cdot H_2O$[41]	Spin-crossover	*ca.* 80% High-spin ?[d]	85.6; 86.7[c]	176.5(5); 178.3(6)[c]	52(2); 52(2)[c]	84; 100[c]
$[Fe(qsal)_2][Ni(dmise)_2] \cdot x CH_3CN$[42]	Spin-crossover	High-spin	89.3	166.35(11)	71.5(4)	207
		Low-spin	89.0	176.59(11)	41.6(4)	67
$[Fe(qsal)_2][Ni(dddt)_2] \cdot CH_3CN \cdot CH_3OH \cdot H_2O$[33]	Partial spin-crossover	High-spin	89.4	165.2(3)	74(1)	217
$[Fe(qnal)_2][Pd(dmit)_2]_5 \cdot (CH_3)_2CO$[43]	Spin-crossover	High-spin	85.9	167.6(2)	74.0(7)	213
		Low-spin	86.5	176.1(3)	40.5(9)	69
$[Fe(qsal)_2]I_3$[44]	Spin-crossover	*ca.* 80 % High-spin	83.7	165.9(2)	65.4(9)	201
		Low-spin	82.9	175.1(2)	39.0(9)	70
$[Fe(5\text{-}Cl\text{-}qsal)_2][Ni(\alpha\text{-}tpdt)_2] \cdot CH_3CN$[45]	Spin-crossover	Low-spin	89.7	177.5(2)	45.0(6)	65
$[Fe(3\text{-}OMe\text{-}qsal)_2]PF_6$[46]	Low-spin	Low-spin	87.4	177.94(18)	48.1(6)	70
$[Fe(qsal)_2]N_3$[47]	Low-spin	Low-spin	89.6	177.62 (7)	53.89(18)	76

[a]Although the anhydrous solids undergo spin-crossover, and are isostructural with the hydrate crystals by powder diffraction, the freshly prepared hydrate crystals remain high-spin on cooling to 5 K.[35] [b]This structure is not deposited on the Cambridge Crystallographic Database. [c]There are two unique molecules in the asymmetric unit of this compound, that are both in the same spin state. [d]Although the Mössbauer spectrum and magnetic moment of this material imply it is predominantly high-spin at room temperature, the metric parameters of its crystal structure at the same temperature are more consistent with a predominantly low-spin state.

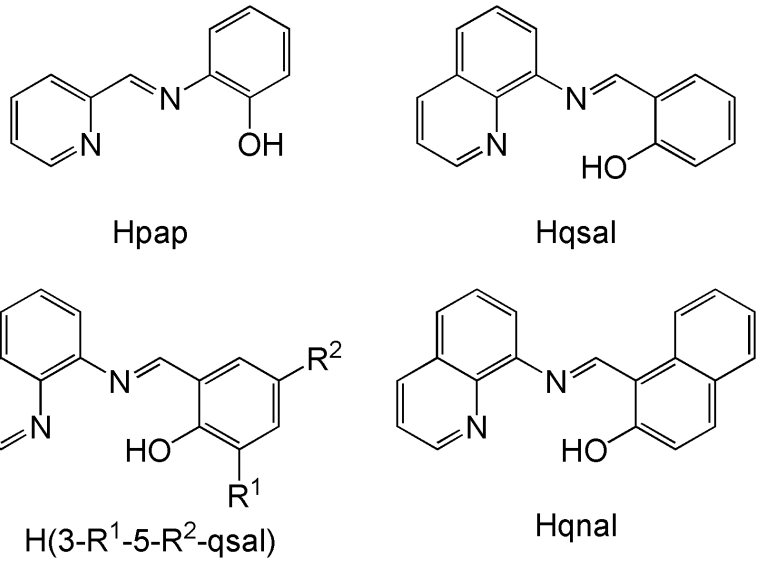

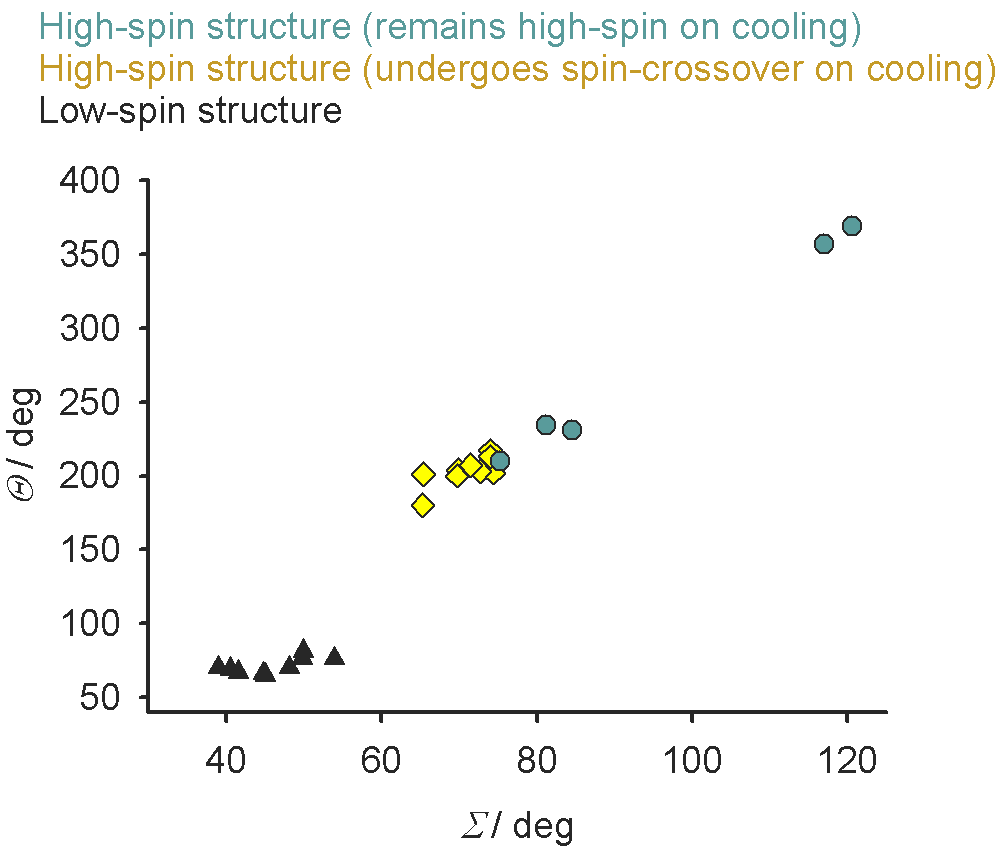

Figure S4. Plot of Σ *vs.* Θ for crystallographically characterised salts of $[Fe(pap)_2]^+$, $[Fe(qsal)_2]^+$ and their derivatives (Table S9).

The twisted ligand conformations adopted by the three high-spin salts of $[Fe(qsal)_2]^+$ have only a small effect on their coordination geometry, expressed using Σ *vs.* Θ.

The outlying points with very high values for these parameters correspond to the two $[Fe(pap)_2]^+$ salts in Table S6, whose exclusively five-membered chelate rings lead to a more distorted coordination geometry.

Table S10 Structural changes taking place during spin-crossover for salts of $[Fe(qsal_2]^+$ and its derivatives, whose high-spin and low-spin crystal structures are available (Table S9, Fig. S4).

	$T_{½}$ (K)	ΔT (K)	$\lvert\Delta\theta\rvert$ (º)	$\lvert\Delta\phi\rvert$ (º)	$\Delta\Sigma$ (º)	$\Delta\Theta$ (º)
$[Fe(qsal)_2][Ni(dmit)_2]\cdot x CH_3CN$[40]	213	37[a]	1.9	10.3	27.9	137
$[Fe(qsal)_2][Ni(dmise)_2]\cdot x CH_3CN$[42]	249	15	0.3	10.24(15)	29.9(6)	140
$[Fe(qsal)_2]I_3$[44]	240	0	0.8[b]	9.2(3)[b]	26.4(13)[b]	131[b]
$[Fe(qnal)_2][Pd(dmit)_2]_5\cdot(CH_3)_2CO$[43]	*ca.* 220	0	0.6	8.5(4)	33.5(11)	144

[a]On the first thermal cycle only. Hysteresis is lost on repeated cyclic about the transition, probably because of solvent loss and/or a crystallographic phase change. [b]May be underestimated, as the high-spin crystal structure appears to have a residual low-spin component.

Table S11 Structural data for iron(II) complexes of Jäger Schiff base ligands. See the next page for schematics of the ligands in this Table, and the main text for the definitions of β, Σ, Θ and the ligand conformations.

	Spin-state behaviour	Spin-state of crystal structure	Ligand conformation	β (°)	Axial *trans*-N–Fe–N (°)	Σ (°)	Θ (°)
$[Fe(L^1)(1\text{-MeIm})_2]$[48]	High-spin	High-spin	*meso*	19.1, 23.4	172.4(8)	70.9(2)	218
$[Fe(L^1)(2\text{-MeIm})_2]$[48]	High-spin	High-spin	umbrella	14.2, 25.3	164.93(7)	86.3(2)	235
$[Fe(L^1)(PyNMe_2)_2]$[49]	High-spin	High-spin	umbrella	21.5, 26.3	169.1(2)	69.6(5)	208
catena-$[Fe(L^2)(\mu\text{-}4,4'\text{-bipy})]\cdot dmf$[49]	High-spin	High-spin	2x *meso*[a]	3.9, 9.3; 5.2, 8.4[a]	177.0(1); 177.3(1)[a]	48.9(4); 46.1(4)[a]	155; 148[a]
catena-$[Fe(L^2)(\mu\text{-}4,4'\text{-dpa})]\cdot C_2H_5OH$ [49]	High-spin	High-spin	*meso*	10.7, 11.6	169.45(9)	64.9(3)	216
catena-$[Fe(L^1)(\mu\text{-bimm})]\cdot ½CH_3OH$[50]	High-spin	High-spin	envelope	5.7, 7.0	167.52(6)	69.36(17)	212
$[Fe(L^4)(1\text{-MeIm})_2]\cdot CH_3OH$ [51]	igh-spin	High-spin	*meso*	6.5, 18.9	176.6(1)	48.9(4)	160
$[Fe_2(\mu\text{-}L^7)(1\text{-MeIm})_4]\cdot 4(1\text{-MeIm})$[49]	High-spin	High-spin	*meso*	10.0, 23.0	173.94(9)	62.5(3)	188
$[Fe(L^1)(Im)_2]$[52]	Spin-crossover	High-spin	umbrella	6.8, 10.8	173.9(1)	54.0(4)	167
$[Fe(L^1)(PyPh)_2]$[53]	S in-crossover	High-spin	envelope	5.2, 7.7	174.47(9)	50.6(2)	163
		Low-spin	envelope	4.2, 6.5	174.7(1)	23.0(3)	59
$[Fe(L^1)(PyCN)_2]\cdot ¼PyCN$[54]	Spin-crossover	High-spin	2x envelope[a]	2.8, 4.6; 3.4, 17.9[a]	176.1(1); 173.8(1)[a]	41.6(3); 44.7(3)[a]	146;146[a]
		Low-spin	2x envelope[a]	3.1, 3.7; 2.4, 15.7[a]	176.1(1); 174.7(1)[a]	21.3(3); 24.6(3)[a]	63; 69[a]
$[Fe(L^2)(Py)_2]$[55]	Spin-crossover	High-spin	envelope	8.3, 11.0	175.6(1)	50.6(2)	162
		Low-Spin	envelope	5.5, 6.7	176.1(1)	21.9(2)	63
$[Fe(L^2)(PyNMe_2)_2]$[55]	Spin-crossover	High-spin	*meso*	7.6, 12.5	171.4(2)	60.7(5)	189
$[Fe(L^2)(1\text{-MeIm})_2]\cdot dmf$[48]	Spin-crossover	High-spin	envelope	5.4, 12.4	177.59(8)	53.0(2)	154
$[Fe(L^2)(1\text{-MeIm})_2]\cdot 1\text{-MeIm}$ [56]	Spin-crossover	High-spin	envelope	8.2, 10.2	179.24(8)	47.1(3)	127
		Low-spin	envelope	1.2, 8.4	179.0(1)	22.9(3)	45
$[Fe(L^2)(PyPh)_2]\cdot PyPh$[53]	Spin-crossover	Low-spin	*meso*	1.5, 4.4	174.84(9)	26.9(3)	67
catena-$[Fe(L^3)(\mu\text{-bimm})]$[57]	Spin-crossover	High-spin	umbrella	16.7, 27.4	171.44(11)	61.6(3)	199
		Low-spin	umbrella	13.6, 21.7	175.21(13)	25.6(5)	74
$[Fe(L^5)(Py)_2]\cdot Py$[58]	Spin-crossover	Low-spin	umbrella	11.5, 14.9	178.49(7)	21.7(2)	38
$[Fe(L^5)(PyNMe_2)_2]\cdot CH_3OH\cdot ½PyNMe_2$[58]	Spin-crossover	Low-spin	umbrella	6.0, 11.6	176.3(2)	20.1(4)	65
catena-$[Fe(L^6)(\mu\text{-}PyC_3H_6Py)]\ ]\cdot ½CH_3OH$ [57]	Partial SCO	High-spin	umbrella	9.8, 10.2	177.26(5)	41.3(2)	141
$[Fe_2(\mu\text{-}L^7)(Py)_4]\cdot 4Py$[59]	Partial SCO[b]	High-spin	envelope	4.6, 14.3	174.4	54.9	176
$[Fe_2(\mu\text{-}L^8)(Py)_4]\cdot 7Py$, high-T phase[59]	Spin-crossover	High-spin	umbrella	11.2, 12.4	170.7	62.7	197
$[Fe_2(\mu\text{-}L^8)(Py)_4]\cdot 7Py$, low-T phase, molecule A[59][c]	n/a	High-spin	2x umbrella	4.8, 7.6; 16.4, 19.8[d]	170.5; 170.0[d]	66.9; 68.9[d]	204; 210[d]
$[Fe_2(\mu\text{-}L^8)(Py)_4]\cdot 7Py$, low-T phase, molecule B[59][c]	Spin-crossover	Low-spin	2x umbrella	9.7, 12.4; 8.9, 9.9[d]	173.8; 174.3[d]	25.5; 28.6[d]	72; 75[d]
$[Fe_2(\mu\text{-}L^8)(1\text{-MeIm})_4]\cdot 4(1\text{-MeIm})$ [56]	Spin-crossover	Low-spin	envelope	2.5, 5.1	178.1(1)	17.8(3)	46

[a]There are two unique molecules in the asymmetric unit of this compound, that are both in the same spin state. [b]This compound remains predominantly high-spin on cooling but shows evidence of spin-crossover involving a fraction of the sample. [c]There are two unique molecules in the asymmetric unit of this phase, which have different spin-state behaviour. [d]The two iron centres in this dinuclear molecule are crystallographically distinct.

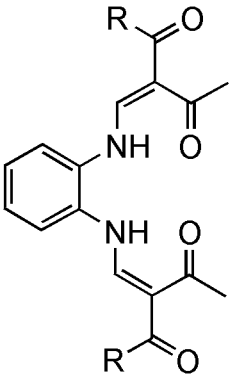

R = OEt, H_2L^1
R = Me, H_2L^2
R = Ph, H_2L^3

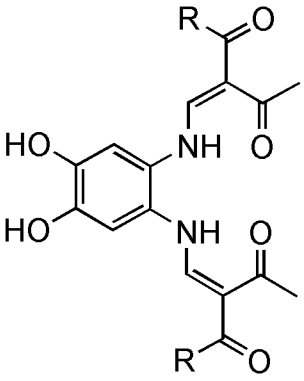

R = OEt, H_2L^4
R = Me, H_2L^5

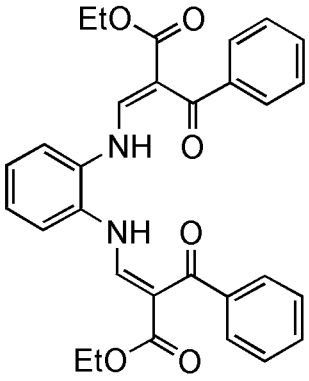

H_2L^6

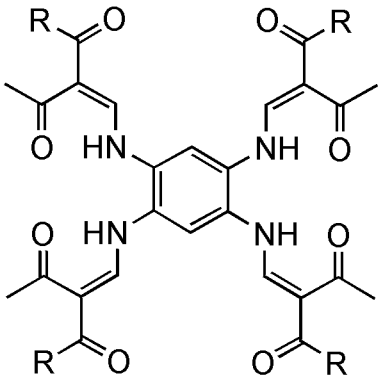

R = OEt, H_4L^7
R = Me, H_4L^8

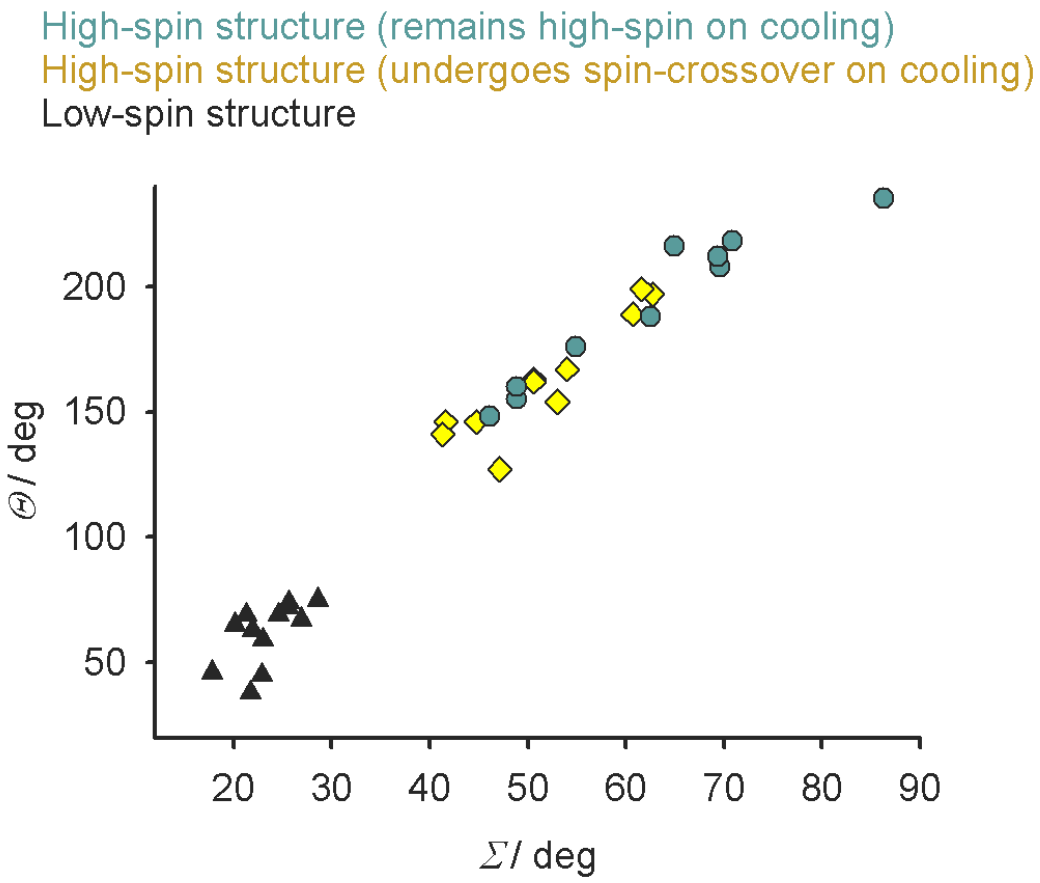

Figure S5 Plot of Σ *vs.* Θ for crystallographically characterised iron(II) complexes of Jäger Schiff base ligands (Table S11).

There is no apparent correlation between Σ and Θ and the degree of conformational twisting in the Jäger chelate (β, Table S7). The high-spin complexes with the most distorted coordination geometries have *trans* N–Fe–N angles to their axial donors that differ strongly from linearity.

Table S12 Structural changes taking place during spin-crossover for iron(II) complexes of Jäger Schiff base ligands, whose high-spin and low-spin crystal structures are available (Table S11, Fig. S5).

	$T_{½}$ (K)	ΔT (K)	$\lvert\Delta\beta\rvert$ (º)	$\lvert\Delta${Axial *trans*-N–Fe–N}$\rvert$ (º)	$\Delta\Sigma$ (º)	$\Delta\Theta$ (º)
$[Fe(L^1)(PyPh)_2]$[53]	234	4	1.1	0.23	27.6	104
$[Fe(L^1)(PyCN)_2]\cdot¼PyCN$[54]	275	0	0.6	0	20.3	83
	175	0 (8[a])	1.6	0.9	20.1	77
$[Fe(L^2)(Py)_2]$[55]	190	2	3.6	0.5	28.7	99
$[Fe(L^2)(1\text{-MeIm})_2]\cdot 1\text{-MeIm}$[56]	178	0	4.0	0.2	24.2	82
catena-$[Fe(L^3)(\mu\text{-}4,4'\text{-bimm})]$	173	5	4.4	3.8	36.0	125

[a]This half-transition takes place in two stages; the second lower-temperature step exhibits an 8 K hysteresis.

Table S13 Structural parameters for iron(II) complexes of tren-based podands. See below for schematics of the ligands in this Table. Data are from ref. [60] unless otherwise stated.

	Spin-state behaviour	Spin-state of crystal structure	Fe–N{bridgehead} (Å)	Σ	Θ
$[Fe(Pz_3tren)][BF_4]_2 \cdot H_2O$	High-spin	High-spin	2.7320(19)	111.5(2)	228
$[Fe(Pz_3tren)][ClO_4]_2 \cdot H_2O$	High-spin	High-spin	2.7468(16)	112.3(2)	229
$[Fe(\{1\text{-}CPh_3\text{-}4\text{-}Im\}_3tren)][PF_6]_2$	High-spin	High-spin	3.004(8)	100.2(12)	241
$[Fe(\{2\text{-}Ph\text{-}4\text{-}Im\}_3tren)][NO_3]_2$	High-spin	High-spin	3.261(7)	83.5(10)	181
$[Fe(Py_3Crypt)][ClO_4]_2$	High-spin above 80 K	High-spin	3.280(3)	99.9(3)	203
$[Fe(\{2\text{-}Me\text{-}4\text{-}Im\}_3tren)]Br[PF_6] \cdot CH_3OH$[61]	High-spin	High-spin	2.991	90.1(2)	200
$[Fe(\{2\text{-}Me\text{-}4\text{-}Im\}_3tren)]Br[AsF_6] \cdot CH_3OH$[61]	High-spin	High-spin	2.997	89.5(2)	200
$[Fe(\{2\text{-}Me\text{-}4\text{-}Im\}_3tren)]Br[SbF_6] \cdot CH_3OH$[61]	High-spin	High-spin	2.995	89.6(3)	199
$[Fe(\{1\text{-}Me\text{-}2\text{-}Im\}_3tren)][PF_6]_2$	n/a	High-spin	2.724(4)	109.9(7)	219
$[Fe(\{1\text{-}Me\text{-}2\text{-}Im\}_3tren)][ClO_4]_2 \cdot CH_3CN$	n/a	High-spin	2.834(3)	123.8(3)	260
$[Fe(\{6\text{-}MePy\}_3tren)][ClO_4]_2$[62]	Spin-crossover	High-spin	3.210 (3)	111(1)	191
		Low-spin	3.572 (1)	83.8(5)	121
$[Fe(\{6\text{-}Me\text{-}5\text{-}(OC_6H_{13})Py\}_3tren)][ClO_4]_2$[63]	Spin-crossover	High-spin	3.162	116.6(4)	196
		Low-spin	3.519	82.1(2)	117
$[Fe(Pz_3tren)][NO_3]_2 \cdot CH_3NO_2$	Spin-crossover	High-spin	2.959(3)	90.1(3)	218
		Low-spin	3.433(1)	65.1(4)	154
$[Fe(Py_3tren)][PF_6]_2$, SCO polymorph	Spin-crossover	High-spin	2.753(8)	n/a	n/a
$[Fe(4\text{-}Im_3tren)][BF_6]_2 \cdot 3H_2O$	Spin-crossover	High-spin	2.889(7)	103.6(6)	220
		Low-spin	3.523(2)	54.6(5)	139
$[Fe(\{2\text{-}Me\text{-}4\text{-}Im\}_3tren)]Cl[I_3]$	Spin-crossover	High-spin	3.085(4)	80.9(5)	195
$[Fe(\{2\text{-}Me\text{-}4\text{-}Im\}_3tren)]Cl[PF_6]$, high-T phase	Spin-crossover	High-spin	3.004(3)	83.5(3)	192
$[Fe(\{2\text{-}Me\text{-}4\text{-}Im\}_3tren)]Cl[PF_6]$, low-T phase, molecule 1[b]	High-spin	High-spin	2.982(1)	82.1(3)	188
$[Fe(\{2\text{-}Me\text{-}4\text{-}Im\}_3tren)]Cl[PF_6]$, low-T phase, molecule 2[b]	Spin-crossover	Low-spin	3.376(1)	61.1(3)	105
$[Fe(\{2\text{-}Me\text{-}4\text{-}Im\}_3tren)]Cl[AsF_6]$	Spin-crossover	High-spin	2.983(4)	83.0(3)	186
		Low-spin	3.372(9)	68.3(14)	118
$[Fe(\{2\text{-}Me\text{-}4\text{-}Im\}_3tren)]Cl[SbF_6]$	Spin-crossover	High-spin	3.017(2)	83.8(3)	182
		Low-spin	3.350(1)	62.6(2)	112
$[Fe(\{2\text{-}Me\text{-}4\text{-}Im\}_3tren)]Cl[CF_3SO_3]$	Spin-crossover	High-spin	2.969(2)	83.0(3)	192
$[Fe(\{2\text{-}Me\text{-}4\text{-}Im\}_3tren)]Br[CF_3SO_3]$[61]	Spin-crossover	High-spin	2.950	84.1(2)	192
		Mostly low-spin	3.228	63.9(4)	138
$[Fe(\{5\text{-}Me\text{-}4\text{-}Im\}_3tren)][ClO_4]_2$	Spin-crossover	High-spin	3.050(3)	94.7(5)	229
$[Fe(2\text{-}Im_3tren)][BF_4]_2 \cdot H_2O$[64]	Spin-crossover	High-spin	2.976(2)	98.7(2)	223
		Low-spin	3.473(1)	54.43(19)	135
$[Fe(2\text{-}Im_3tren)][ClO_4]_2 \cdot H_2O$	Spin-crossover	Low-spin	3.437(1)	59.0(3)	130
		Low-spin	3.527(1)	54.3(3)	132

Table S13 continued

$[Fe(2\text{-}Im_3tren)]Cl_{0.5}[PF_6]_{1.5}\cdot 2H_2O$	n/a	Low-spin	3.441	56.3	128
$[Fe(\{1\text{-}Me\text{-}2\text{-}Im\}_3tren)]I_2$[65]	n/a	Low-spin	3.437(3)	57.1(4)	144
$[Fe(\{1\text{-}allyl\text{-}2\text{-}Im\}_3tren)]I_2$[65]	n/a	Low-spin	3.363(6); 3.364(6); 3.485(6)[c]	61(1); 56(1); 54(1)[c]	135; 128; 133[c]
$[Fe(Py_3tren)][BF_4]_2$	Low-spin	Low-spin	3.439	60.3	114
$[Fe(Py_3tren)][ClO_4]_2$	Low-spin	Low-spin	3.477(1)	61.4(2)	110
$[Fe(Py_3tren)][PF_6]_2$, low-spin polymorph	Low-spin	Low-spin	3.435(1)	63.9(5)	114
$[Fe(\{5\text{-}(OC_6H_{13})Py\}_3tren)][ClO_4]_2$[63]	Low-spin	Low-spin	3.417; 3.423[d]	66.7(3); 68.1(3)[d]	113; 109[d]
$NaFe(2\text{-}Im_3tren)][BF_4]_3$[64]	Low-spin	Low-spin	3.413(4)	53.5(3)	123
$K[Fe(2\text{-}Im_3tren)][BF_4]_3$[64]	Low-spin	Low-spin	3.372(2)	56.70(17)	120
$Rb[Fe(2\text{-}Im_3tren)][BF_4]_3$[64]	Low-spin	Low-spin	3.360(4)	57.8(2)	126
$Cs[Fe(2\text{-}Im_3tren)][BF_4]_3$[64]	Low-spin	Low-spin	3.357(5)	57.2(3)	123
$NH_4[Fe(2\text{-}Im_3tren)][BF_4]_3$[64]	Low-spin	Low-spin	3.383(3)	55.35(17)	122
$K[Fe(2\text{-}Im_3tren)][ClO_4]_3$[66]	Low-spin	Low-spin	3.350(1)	58.14(14)	119
$Rb[Fe(2\text{-}Im_3tren)][ClO_4]_2$[66]	Low-spin	Low-spin	3.376(1)	56.28(17)	122
$Cs[Fe(2\text{-}Im_3tren)][ClO_4]_2$[66]	Low-spin	Low-spin	3.386(2)	54.4(3)	122
$NH_4[Fe(2\text{-}Im_3tren)][ClO_4]_2$[66]	Low-spin	Low-spin	3.380(1)	56.31(14)	120

[a]Estimated value based on incomplete published data. [b]There are two unique molecules in the asymmetric unit of this phase, which have different spin-state behaviour. [c]There are three unique molecules in the asymmetric unit of this compound, all in the same spin state. [d]There are two unique molecules in the asymmetric unit of this compound, both in the same spin state.

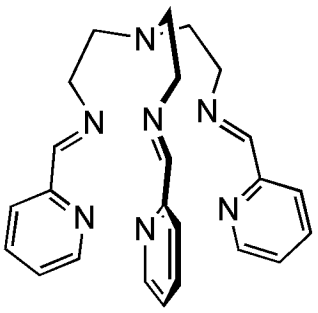

Py_3tren

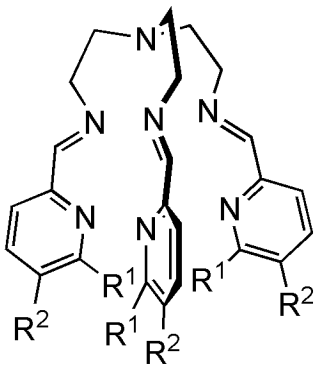

$\{6\text{-}R^1\text{-}5\text{-}R^2\text{-}Py\}_3tren$

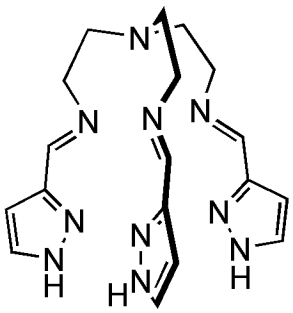

Pz_3tren

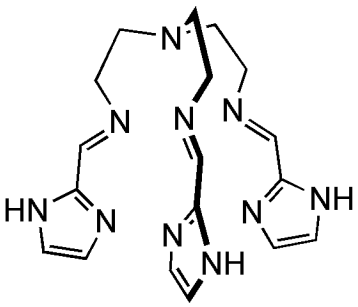

$2\text{-}Im_3tren$

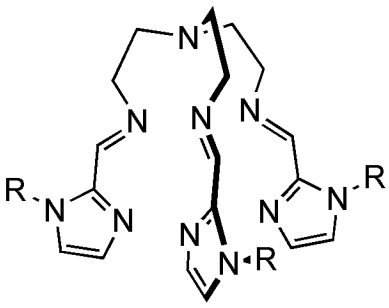

$\{1\text{-}R\text{-}2\text{-}Im\}_3tren$

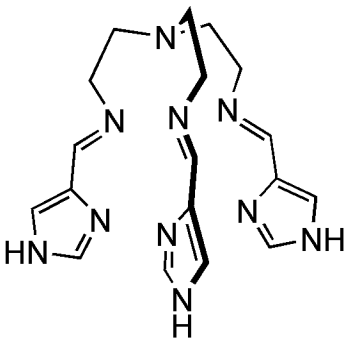

$4\text{-}Im_3tren$

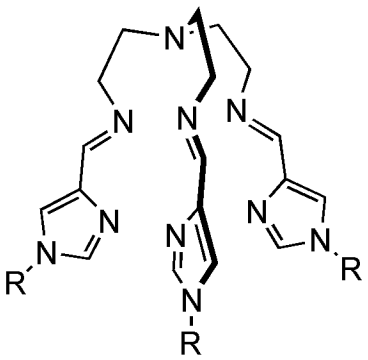

$\{1\text{-}R\text{-}4\text{-}Im\}_3tren$

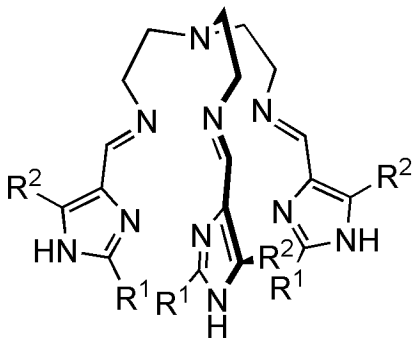

$\{2\text{-}R^1\text{-}5\text{-}R^2\text{-}4\text{-}Im\}_3tren$

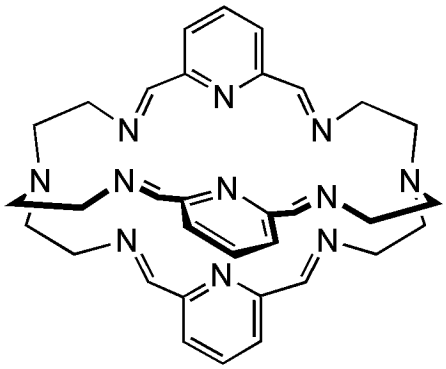

Py_3crypt

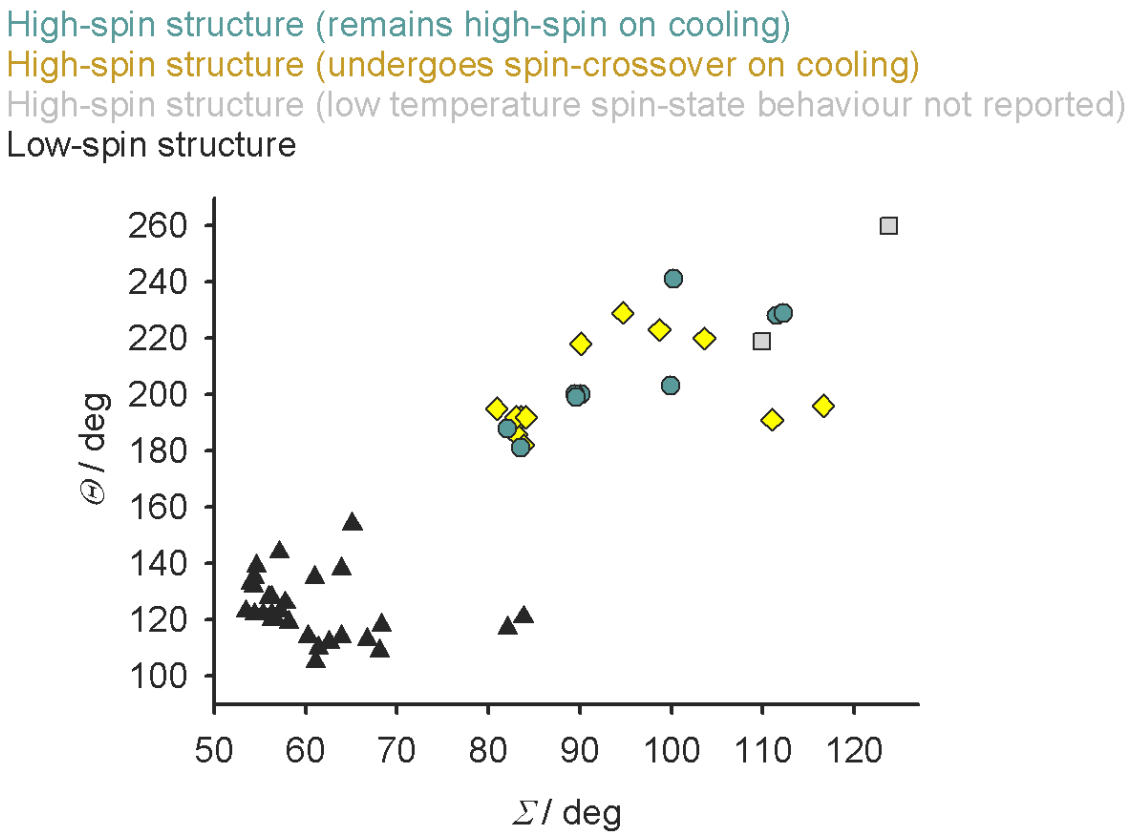

Figure S6 Plot of Σ *vs.* Θ for crystallographically characterised iron(II) complexes of tren-based podands (Table S13).

There is no apparent correlation between Σ and Θ and the occurence of spin-crossover in these compounds.

The two outlying low-spin datapoints with $\Sigma \approx 85°$ are $[Fe(\{6\text{-MePy}\}_3tren)]^{2+}$ derivatives, whose methyl substituents exert a strong steric influence on the metal coordination sphere.

Table S14 Structural changes taking place during spin-crossover for iron(II) complexes of tren-based podands, whose high-spin and low-spin crystal structures are available (Table S13, Fig. 6). Data are from ref. [58] unless otherwise stated.

	$T_{½}$ (K)	ΔT (K)	ΔFe...N{bridgehead} (Å)	$\Delta\Sigma$ (°)	$\Delta\Theta$ (°)
$[Fe(\{6\text{-MePy}\}_3tren)][ClO_4]_2$[61]	233	0	0.362(3)	27(1)	70
$[Fe(\{6\text{-Me-5-}(OC_6H_{13})Py\}_3tren)][ClO_4]_2$[62]	146	0	0.357	34.5(4)	79
$[Fe(Pz_3tren)][NO_3]_2{\cdot}CH_3NO_2$	139	0	0.474(3)	25.0(5)	64
$[Fe(4\text{-}Im_3tren)][BF_6]_2{\cdot}3H_2O$	210	0	0.634(7)	49.0(8)	81
$[Fe(\{2\text{-Me-4-Im}\}_3tren)]Cl[PF_6]$	122	0	0.372(3)	22.4(4)	87
$[Fe(\{2\text{-Me-4-Im}\}_3tren)]Cl[AsF_6]$	97[a]	0	0.39(1)	14.7(3)	68
$[Fe(\{2\text{-Me-4-Im}\}_3tren)]Cl[SbF_6]$	120	0	0.333(2)	21.2(4)	70
$[Fe(\{2\text{-Me-4-Im}\}_3tren)]Br[CF_3SO_3]$[60]	97	2	0.278[b]	20.2(4)[b]	54[b]
$[Fe(\{5\text{-Me-4-Im}\}_3tren)][ClO_4]_2$	n/a	n/a	0.477(3)	40.4(6)	97
$[Fe(2\text{-}Im_3tren)][BF_4]_2{\cdot}H_2O$[61]	n/a	n/a	0.497(2)	54.3(3)	88

[a]Transition proceeds in two closely-spaced steps, in a material with just one unique iron site. The $T_{½}$ value is the temperature where the transition has proceed to 50% completion in the material as a whole. [b]May be underestimated, as the low-spin crystal structure appears to have a residual high-spin component.

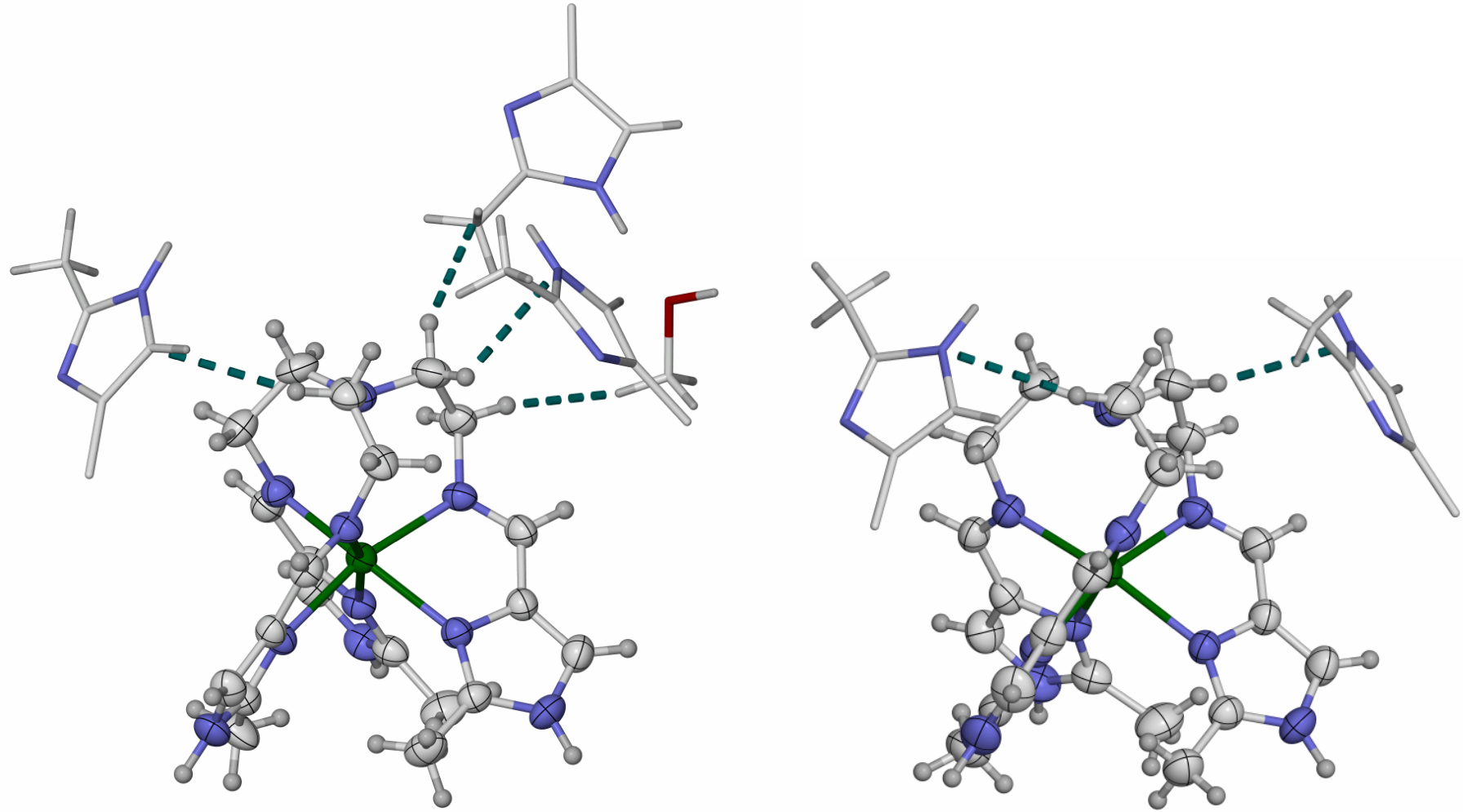

Figure S7. Close intermolecular contacts involving the capping $N(C_2H_4)_3$ moiety in high-spin [Fe({2-Me-4-Im}$_3$tren)]Br[AsF_6]·CH_3OH (left) and in spin-crossover [Fe({2-Me-4-Im}$_3$tren)]Br[CF_3SO_3] (right).[60] Only contacts that are equal to, or closer than, the van der Waals radii of the two interacting atoms are shown.

The more crowded steric environment about the capping group may inhibit spin-crossover in the high-spin AsF_6^- salt, and in the isostructural PF_6^- and SbF_6^- crystals. The same argument has previously been made to explain the high-spin nature of some salts of $[Fe(Pz_3tren)]^{2+}$. [58]

References

[1] M. A. Halcrow, *Coord. Chem. Rev.*, 2009, **253**, 2493.
[2] M. Nihei, H. Tahira, N. Takahashi, Y. Otake, Y. Yamamura, K. Saito and H. Oshio, *J. Am. Chem. Soc.*, 2010, **132**, 3553.
[3] I. Šalitroš, J. Pavlik, R. Boča, O. Fuhr, C. Rajadurai and M. Ruben, *CrystEngComm*, 2010, **12**, 2361.
[4] C. A. Tovee, C. A. Kilner, S. A. Barrett, J. A. Thomas and M. A. Halcrow, *Eur. J. Inorg. Chem.*, 2010, 1007.
[5] D. L. Reger, J. R. Gardinier, J. D. Elgin, M. D. Smith, D. Hautot, G. J. Long and F. Grandjean, *Inorg. Chem.*, 2006, **45**, 8862.
[6] T. Kitano, Y. Sohrin, Y. Hata, H. Wada, T. Hori and K. Ueda, *Bull Chem. Soc. Jpn.*, 2003, **76**, 1365.
[7] N. Zhao, M. J. Van Stipdonk, C. Bauer, C. Campana and D. M. Eichhorn, *Inorg. Chem.*, 2007, **46**, 8662.
[8] L. Salmon, G. Molnár, S. Cobo, P. Oulié, M. Etienne, T. Mahfoud, P. Demont, A. Eguchi, H. Watanabe, K. Tanaka and A. Bousseksou, *New J. Chem.*, 2009, **33**, 1283.
[9] P. Hamon, J.-Y. Thépot, M. Le Floch, M.-E. Boulon, O. Cador, S. Golhen, L. Ouahab, L. Fadel, J.-Y. Saillard and J.-R. Hamon, *Angew. Chem., Int. Ed.*, 2008, **47**, 8687.
[10] C. Janiak, S. Temizdemir, S. Dechert, W. Deck, F. Girgsdies, J. Heinze, M. J. Kolm, T. G. Scharmann and O. M. Zipffel, *Eur. J. Inorg. Chem.*, 2000, 1229.
[11] D. L. Reger, C. A. Little, M. D. Smith, A. L. Rheingold, K.-C. Lam, T. L. Concolino, G. J. Long, R. P. Hermann and F. Grandjean, *Eur. J. Inorg. Chem.*, 2002, 1190.
[12] M. A. Tershansy, A. M. Goforth, J. R. Gardinier,1, M. D. Smith, L. Peterson jr. and H.-C. zur Loye, *Solid State Sci.*, 2007, **9**, 410.
[13] D. L. Reger, M. D. Smith and K. J. Brown, *J. Chem. Cryst.*, 2009, **39**, 545.
[14] D. L. Reger, C. A. Little, A.L. Rheingold, M. Lam, L. M. Liable-Sands, B. Rhagitan, T. Concolino, A. Mohan, G. J. Long, V. Briois and F. Grandjean, *Inorg. Chem.*, 2001, **40**, 1508; D. L. Reger, C. A. Little, V. G. Young jr. and M. Pink, *Inorg. Chem.*, 2001, **40**, 2870.
[15] I. Kuzu, I. Krummenacher, I. J. Hewitt, Y. Lan, V. Mereacre, A. K. Powell, P. Höfer, J. Harmer and F. Brehe, *Chem. Eur. J.*, 2009, **15**, 4350.
[16] D. L. Reger, J. D. Elgin, E. A. Foley, M. D. Smith, F. Grandjean and G. J. Long, *Inorg. Chem.*, 2009, **48**, 9393.
[17] D. L. Reger, J. D. Elgin, M. D. Smith, F. Grandjean, L. Rebbouh and G. J. Long, *Eur. J. Inorg. Chem.*, 2004, 3345.
[18] B. Moubaraki, B. A. Leita, G. J. Halder, S. R. Batten, P. Jensen, J. P. Smith, J. D. Cashion, C. J. Kepert, J.-F. Létard and K. S. Murray, *Dalton Trans.*, 2007, 4413.
[19] P. A. Anderson, T. Astley, M. A. Hitchman, F. R. Keene, B. Moubaraki, K. S. Murray, B. W. Skelton, E. R. T. Tiekink, H. Toftlund and A. H. White, *J. Chem. Soc., Dalton Trans.*, 2000, 3505.
[20] D. L. Reger, C. A. Little, A.L. Rheingold, M. Lam, L. M. Liable-Sands, B. Rhagitan, T. Concolino, A. Mohan, G. J. Long, V. Briois and F. Grandjean, *Inorg. Chem.*, 2001, **40**, 1508.
[21] A. A. Salaudeen, C. A. Kilner and M. A. Halcrow, *Polyhedron*, 2008, **27**, 2569.
[22] D. L. Reger, R. F. Semeniuc and M. D. Smith, *Dalton Trans.*, 2008, 2253.
[23] D. L. Reger, C. A. Little, R. F. Semeniuc and M. D. Smith, *Inorg. Chim. Acta*, 2009, **362**, 303.
[24] R. Pritchard, S. A. Barrett, C. A. Kilner and M. A. Halcrow, *Dalton Trans.*, 2008, 3159 and 2009, 10622 (correction).
[25] P. N. Martinho, C. J. Harding, H. Müller-Bunz, M. Albrecht and G. G. Morgan, *Eur. J. Inorg. Chem.*, 2010, 675. The value of α for [Fe(saltrien)]BF_4 should be 104.0(1)°, not 76.0(1)° as given in this paper.
[26] M. Clemente-León, E. Coronado, M. López-Jordà, G. Mínguez Espallargas A. Soriano-Portillo and J. C. Waerenborgh, *Chem. Eur. J.*, 2010, **16**, 2207.
[27] C. Faulmann, P. Á. Szilágyi, K. Jacob, J. Chahine and L. Valade, *New J. Chem.*, 2009, **33**, 1268.
[28] D. Boinnard, A. Bousseksou, A. Dworkin, J.-M. Savariault, F. Varret and J.-P. Tuchagues, *Inorg. Chem.*, 1994, **33**, 271.
[29] L. Salmon, A. Bousseksou, B. Donnadieu and J.-P. Tuchagues, *Inorg. Chem.*, 2005, **44**, 1763.
[30] A. Bousseksou, L. Salmon, F. Varret and J.-P. Tuchagues, *Chem. Phys. Lett.*, 1998, **282**, 209; L. Salmon, B. Donnadieu, A. Bousseksou and J.-P. Tuchagues, *C. R. Acad. Sci. Paris, Ser. IIc*, 1999, **2**, 305.
[31] S. Hayami, T. Matoba, S. Nomiyama, T. Kojima, S. Osaki and Y. Maeda, *Bull. Chem. Soc. Jpn.*, 1997, **70**, 3001.
[32] M. Griffin, S. Shakespeare, H. J. Shepherd, C.J. Harding, J.-F. Létard, C. Desplanches, A. E. Goeta, J. A. K. Howard, A. K. Powell, V. Mereacre, Y. Garcia, A. D. Naik, H. Müller-Bunz and G. G. Morgan, *Angew. Chem. Int. Ed.*, 2011, **5**0, 896.

[33] X.-M. Li, Y. Ji, C.-F. Wang, J.-L. Zuo and X.-Z. You, *J. Coord. Chem.*, 2009, **62**, 1544.
[34] J. C. Dias, A. Soriano-Portillo, M. Clemente-Léon, C. Giménez-Saiz, J. R. Galán-Mascarós, C. J. Gómez-García and E. Coronado, *Inorg. Chim. Acta*, 2007, **360**, 3843.
[35] S. Hayami, K. Hiki, T. Kawahara, Y. Maeda, D. Urakami, K. Inoue, M. Ohama, S. Kawata and O. Sato, *Chem. Eur. J.*, 2009, **15**, 3497.
[36] S. Hayami, Z.-Z. Gu, M. Shiro, Y. Einaga, A. Fujishima and O. Sato, *J. Am. Chem. Soc.*, 2000, **122**, 7126 and 11569 (correction).
[37] G. Juhász, S. Hayami, O. Sato and Y. Maeda, *Chem. Phys. Lett.*, 2002, **364**, 164.
[38] S. Hayami, Z.-Z. Gu, H. Yoshiki, A. Fujishima and O. Sato, *J. Am. Chem. Soc.*, 2001, **123**, 11644.
[39] C. Faulmann, S. Dorbes, S. Lampert a, K. Jacob, B. Garreau de Bonneval, G. Molnár, A. Bousseksou, J. A. Real and L. Valade, *Inorg. Chim. Acta*, 2007, **360**, 3870.
[40] K. Takahashi, H.-B. Cui, H. Kobayashi, Y. Einaga and O. Sato, *Chem. Lett.*, 2005, **34**, 1240.
[41] K. Takahashi, H.-B. Cui, Y. Okano, H. Kobayashi, Y. Einaga and O. Sato, *Inorg. Chem.*, 2006, **45**, 5739.
[42] K. Takahashi, H. Mori, H. Kobayashi and O. Sato, *Polyhedron*, 2009, **28**, 1776.
[43] K. Takahashi, H.-B. Cui, Y. Okano, H. Kobayashi, H. Mori, H. Tajima, Y. Einaga and O. Sato, *J. Am. Chem. Soc.*, 2008, **130**, 6688.
[44] K. Takahashi, T. Sato, H. Mori, H.Tajima and O. Sato, *Physica B*, 2010, **405**, S65.
[45] A. I. S. Neves, J. C. Dias, B. J. C. Vieira, I. C. Santos, M. B. C. Branco, L. C. J. Pereira, J. C. Waerenborgh, M. Almeida, D. Belo and V. da Gama, *CrystEngComm*, 2009, **11**, 2160.
[46] J. C. Dias, B. Vieira, I. C. Santos, L. C.J. Pereira and V. da Gama, *Inorg. Chim. Acta*, 2009, **362**, 2076.
[47] Y. Kojima, K. Kato, Y. Yamamoto, K. Inoue and S. Hayami, *Acta Crystallogr., Sect. E*, 2010, **66**, m204.
[48] B. Weber, E. Kaps, J. Obel and W. Bauer, *Z. Anorg. Allg. Chem.*, 2008, **634**, 1421.
[49] W. Bauer and B. Weber, *Inorg. Chim. Acta*, 2009, **362**, 2341.
[50] T. Pfaffeneder, W. Bauer and B. Weber, *Z. Anorg. Allg. Chem.*, 2010, **636**, 183.
[51] B. Weber and J. Obel, *Z. Anorg. Allg. Chem.*, 2009, **635**, 2474.
[52] B. Weber, W. Bauer and J. Obel, *Angew. Chem., Int. Ed.*, 2008, **47**, 10098.
[53] B. Weber, E. S. Kaps, C. Desplanches, J.-F. Létard, K. Achterhold and F. G. Parak, *Eur. J. Inorg. Chem.*, 2008, 4891.
[54] B. Weber, C. Carbonera, C. Desplanches and J.-F. Létard, *Eur. J. Inorg. Chem.*, 2008, 1589.
[55] B. Weber, E. Kaps, J. Weigand, C. Carbonera, J.-F. Létard, K. Achterhold and F. G. Parak, *Inorg. Chem.*, 2008, **47**, 487.
[56] B. Weber, E. S. Kaps, J. Obel, K. Achterhold and F. G. Parak, *Inorg. Chem.*, 2008, **47**, 10779.
[57] T. M. Pfaffeneder, S. Thallmair, W. Bauer and B. Weber, *New J. Chem.*, 2011, **35**, 691.
[58] B. Weber, J. Obel, D. Henner-Vásquez and W. Bauer, *Eur. J. Inorg. Chem.*, 2009, 5527.
[59] B. Weber and E. Kaps, *Heteroatom Chem.*, 2005, **16**, 391.
[60] H. Z. Lazar, T. Forestier, S. A. Barrett, C. A. Kilner, J.-F. Létard and M. A. Halcrow, *Dalton Trans.*, 2007, 4276.
[61] H. Hagiwara, N. Matsumoto, S.Iijima and M. Kojima, *Inorg. Chim. Acta*, 2011, **366**, 283.
[62] M. Seredyuk, A. B. Gaspar, J. Kusz, G. Bednarek and P. Gütlich, *J. Appl. Cryst.*, 2007, **40**, 1135.
[63] M. Seredyuk, A. B. Gaspar, V. Ksenofontov, Y. Galyametdinov, J. Kusz and P. Gütlich, *J. Am. Chem. Soc.*, 2008, **130**, 1431.
[64] L. Alvarado, C. Brewer, G. Brewer, R. J. Butcher, A. Straka and C. Viragh, *CrystEngComm*, 2009, **11**, 2297.
[65] G. Brewer, C. Brewer, R. J. Butcher, E. E. Carpenter, L. May and G. White, *Inorg. Chim. Acta*, 2007, **360**, 2153.
[66] G. Brewer, R. J. Butcher, C. Viragh and G.White, *Dalton Trans.*, 2007, 4132.